



# Cyanobacteria as Natural Therapeutics and Pharmaceutical Potential: Role in Antitumor Activity and as Nanovectors

Hina Qamar, Kashif Hussain, Aishwarya Soni, Anish Khan, Touseef Hussain, Benoit Chénais

## ► To cite this version:

Hina Qamar, Kashif Hussain, Aishwarya Soni, Anish Khan, Touseef Hussain, et al.. Cyanobacteria as Natural Therapeutics and Pharmaceutical Potential: Role in Antitumor Activity and as Nanovectors. *Molecules*, 2021, 26, 10.3390/molecules26010247 . hal-03106367

**HAL Id: hal-03106367**

**<https://univ-lemans.hal.science/hal-03106367>**

Submitted on 11 Jan 2021

**HAL** is a multi-disciplinary open access archive for the deposit and dissemination of scientific research documents, whether they are published or not. The documents may come from teaching and research institutions in France or abroad, or from public or private research centers.

L'archive ouverte pluridisciplinaire **HAL**, est destinée au dépôt et à la diffusion de documents scientifiques de niveau recherche, publiés ou non, émanant des établissements d'enseignement et de recherche français ou étrangers, des laboratoires publics ou privés.

## Review

# Cyanobacteria as Natural Therapeutics and Pharmaceutical Potential: Role in Antitumor Activity and as Nanovectors

Hina Qamar <sup>1</sup>, Kashif Hussain <sup>2,3</sup>, Aishwarya Soni <sup>4</sup>, Anish Khan <sup>5</sup>, Touseef Hussain <sup>6,\*</sup> and Benoît Chénais <sup>7,\*</sup>

<sup>1</sup> Interdisciplinary Biotechnology Unit, Aligarh Muslim University, Aligarh 202002, India; hina.dna@rediffmail.com

<sup>2</sup> Pharmacy Section, Gyani Inder Singh Institute of Professional Studies, Dehradun 248003, India; kashif@gisips.com

<sup>3</sup> School of Pharmacy, Glocal University, Saharanpur 247121, India

<sup>4</sup> Department of Biotechnology, Deenbandhu Chhotu Ram University of Science and Technology, Murthal, Sonapat 124001, India; aishwaryasoni32@gmail.com

<sup>5</sup> Centre for Biotechnology, Maharshi Dayanand University, Rohtak 124001, India; anishkhan.rs.biotech@mdurohtak.ac.in

<sup>6</sup> Department of Botany, Aligarh Muslim University, Aligarh 202002, India

<sup>7</sup> EA 2160 Mer Molécules Santé, Le Mans Université, F-72085 Le Mans, France

\* Correspondence: hussaintouseef@yahoo.co.in (T.H.); bchenais@univ-lemans.fr (B.C.); Tel.: +33-243-833251 (B.C.)

**Abstract:** Cyanobacteria (blue-green microalgae) are ubiquitous, Gram-negative photoautotrophic prokaryotes. They are considered as one of the most efficient sources of bioactive secondary metabolites. More than 50% of cyanobacteria are cultivated on commercial platforms to extract bioactive compounds, which have been shown to possess anticancer activity. The chemically diverse natural compounds or their analogues induce cytotoxicity and potentially kill a variety of cancer cells via the induction of apoptosis, or altering the activation of cell signaling, involving especially the protein kinase-C family members, cell cycle arrest, mitochondrial dysfunctions and oxidative damage. These therapeutic properties enable their use in the pharma and healthcare sectors for the betterment of future generations. This review provides a baseline overview of the anti-cancerous cyanobacterial bioactive compounds, along with recently introduced nanomaterials that could be used for the development of new anticancer drugs to build a healthy future for mankind.

**Keywords:** cyanobacteria; bioactivity; natural compounds; anti-tumor; cytotoxicity; secondary metabolites; nanoparticles



**Citation:** Qamar, H.; Hussain, K.; Soni, A.; Khan, A.; Hussain, T.; Chénais, B. Cyanobacteria as Natural Therapeutics and Pharmaceutical Potential: Role in Antitumor Activity and as Nanovectors. *Molecules* **2021**, *26*, 247. <https://doi.org/10.3390/molecules26010247>

Received: 25 October 2020

Accepted: 14 December 2020

Published: 5 January 2021

**Publisher's Note:** MDPI stays neutral with regard to jurisdictional claims in published maps and institutional affiliations.



**Copyright:** © 2021 by the authors. Licensee MDPI, Basel, Switzerland. This article is an open access article distributed under the terms and conditions of the Creative Commons Attribution (CC BY) license (<https://creativecommons.org/licenses/by/4.0/>).

## 1. Introduction

Cyanobacteria (blue-green microalgae) are ubiquitous Gram-negative photoautotrophic prokaryotes, for which evidence they existed 3.3–3.5 billion years ago was found [1]. They exist in the environment as unicellular, filamentous or colonial forms surrounded by a mucilaginous sheath [2]. Owing to their ubiquitous nature and the vast diversity of their metabolites, they have several applications in the biomedical field. During the last few decades, the emergence of new cancers and their developing resistance to available drugs has led to chemotherapeutic failure. Thus, the identification of new biologically active compounds is immediately required for the development of new drugs. In this regard, the medicinal properties of cyanobacteria have been explored. To date, several secondary metabolites have been isolated from the members of oscillatoriiales (49%), followed by nostocales (26%), chroococcales (16%), pleurocapsales (6%) and stigonematales (4%) [2,3]. The capacity of cyanobacteria to integrate non-ribosomal peptide synthetases with polyketide synthases enables them to produce biologically active and chemically diverse compounds,

such as cyclic alkaloids, peptides, depsipeptides, cyclic depsipeptides, fatty acid, lipopeptides, swinholides and saccharides [4]. Back in 1500 BC, *Nostoc* sp. was first used to treat gout, fistula and different types of cancers [5]. However, more focused research utilizing modern technologies was started in this field in the 1990s. Several cyanobacteria species are cultivated in commercial platforms to extract bioactive compounds, which have been shown to possess anticancer activity and potentially kill a variety of cancer cells via the induction of apoptosis or altering the activation of cell signaling [4,6] (Figure 1).

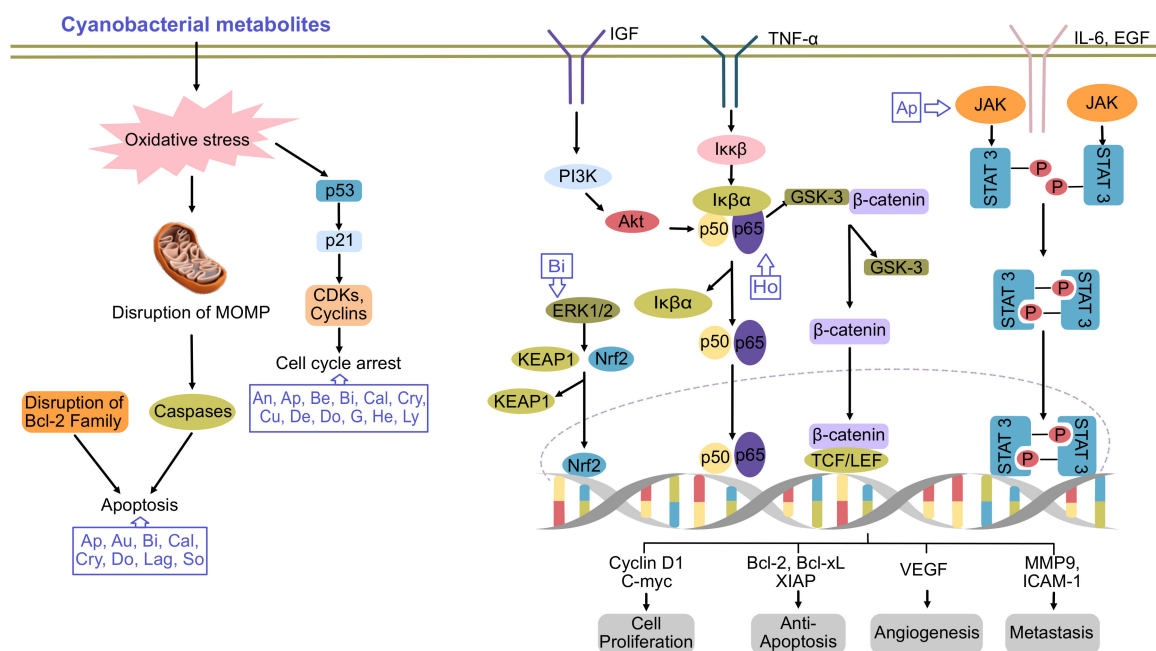


**Figure 1.** Major pathways of cancer inhibited by cyanobacterial metabolites. An, ankarholide; Ap, apratoxin; Au, aurilide; Be, belamide A; Bi, bisebromoamide; Cal, calothrixin A; Cry, cryptophycin; Cu, curacin A; De, desmethoxymajusculamide; Do, dolastatins; G, grassystatin; He, heterochlorin; Ho, hoiamide; Lag, lagunamide; Lyn, lyngbyabellin; So, somocystinamide A. Adapted and enhanced from [7].

## 2. Anticancer Potential of Bioactive Compounds from Cyanobacteria

### 2.1. Ankaraholide A

Ankaraholide A (Figure 2), a glycosylated swinholides isolated from *Geitlerinema*, repressed proliferation in the mouse neuroblastoma cell line Neuro-2a, the human lung cancer cell line NCI-H460, and the human melanoma cell line MDA-MB-435, with  $IC_{50}$  values of 119 nM, 262 nM and 8.9 nM, respectively (Table 1). Furthermore, in the rat non-tumoral myoblast A-10 cells, it caused a complete loss of the filamentous (F)-actin at the 30 nM and 60 nM concentrations [8].

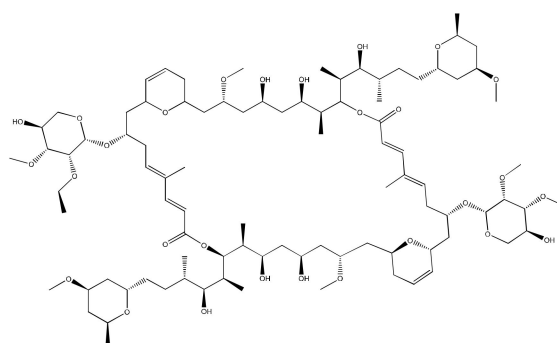


**Figure 2.** Chemical structure of Ankaraholide A.

## 2.2. Apratoxin

Apratoxin, a cyclic depsipeptide isolated from *Micronesia* and *Lyngbya* sp., is a potent cytotoxic marine natural product that showed anti-cancerous activity against various cancer cell lines (Table 1). Apratoxin has antiproliferative effects via the induction of G1 cell cycle arrest and apoptotic cascade [9]. Furthermore, it inhibits the Janus kinase (JAK)/signal transducer and activator of transcription (STAT) signaling pathway by downregulating the interleukin (IL)-6 molecule signal transducer (gp130) and reversibly inhibiting the secretory pathway by preventing cotranslational translocation early in the secretory pathway [10]. Apratoxin A (Figure 3), isolated from *Lyngbya* sp., induces cytotoxicity on adenocarcinoma cells, and showed cytotoxicity in the nanomolar range when tested against HT29 (colorectal adenocarcinoma), HeLa (cervix adenocarcinoma) and U2OS (osteosarcoma) cancer cell lines. The  $IC_{50}$  value ranges from 0.36 to 0.52 nM for in vitro studies while, for in vivo studies it was only marginally active against a colon tumor, and was ineffective against a mammary tumor [11]. Furthermore, apratoxin also affects the apoptosis of cancer cells by downregulating receptors and the associated growth ligand. A hybrid synthetic molecule that combines both apratoxins A and E has been synthesized with improved in vivo antitumor properties. It downregulated receptor tyrosine kinases and vascular endothelial growth factor A (VEGF-A) in a colorectal tumor xenograft model [12]. Oxazoline, a synthetic analogue of apratoxin A, inhibits the function of heat shock protein 90 (Hsp90) and promotes chaperone-mediated autophagy [13]. The in vivo pathological studies against the pancreatic tumor revealed that the Sec 61 complex is the molecular target of apratoxin A [14]. Recently, apratoxin S10 (Apra S10, an apratoxin A analogue) has been developed, which induced promising antitumor effects in the pancreatic cancer model by exhibiting the downregulation of multiple receptor tyrosine kinases and inhibiting several growth factors and cytokine secretion [15]. Moreover, apratoxin D revealed strong cytotoxicity, with an  $IC_{50}$  value of 2.6 nM against NCI-H460 lung cancer cells [16].

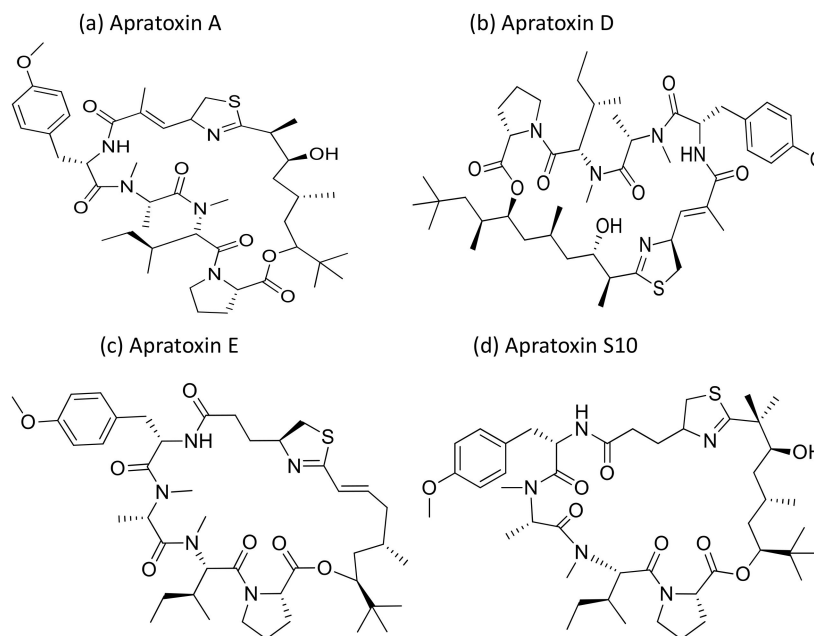


**Figure 3.** Chemical structures of apratoxins.

## 2.3. Aurilide

Aurilide, a cyclic depsipeptide isolated from *Dolabella auricularia*, showed cytotoxicity ranging from picomolar (pM) to nanomolar (nM) concentrations against several cancer cell lines (Table 1) [17]. It encourages mitochondrial-induced apoptosis by selectively binding to prohibitin 1 (PHB1) in the mitochondria and activating the proteolytic processing of optic atrophy 1 (OPA1) [18]. Aurilides B and C (aurilide analogues, Figure 4) showed



in vitro cytotoxicity against an NCI-H460 human lung tumor and the neuro-2a mouse neuroblastoma cell lines, with  $LC_{50}$  values ranging from 0.01 to 0.13  $\mu$ M [17]. Aurilide B exhibits potent cytotoxicity against human renal, leukemia and prostate cancer cell lines from the NCI-60 panel, a panel of 60 different human tumor cell lines of different tissue origins, with an average growth inhibition ( $GI_{50}$ ) value of less than 10 nM [17].

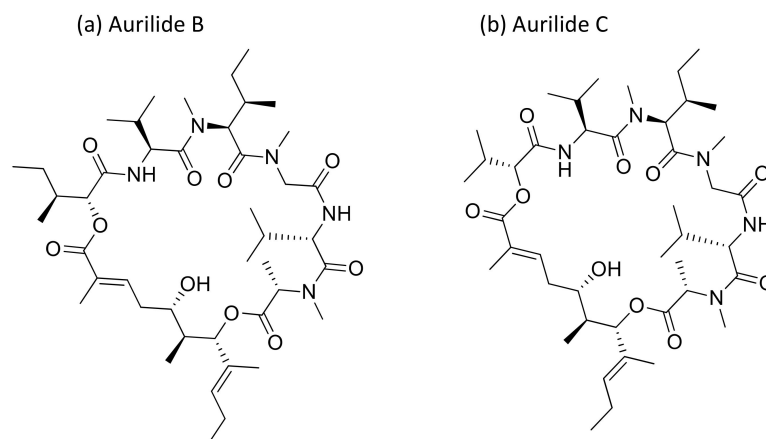


**Figure 4.** Chemical structure of aurilide analogs.

#### 2.4. Bisebromoamide

Bisebromoamide (Figure 5), a linear peptide isolated from an Okinawan strain of *Lyngbya* sp., contains a unique N-methyl-3-bromotyrosine, a modified 4-methylproline, a 2-(1-oxopropyl) pyrrolidine and an N-pivalamide unit. Based on cell morphological profiling analysis, bisebromoamide was identified as an actin filament stabilizer [19]. It revealed cytotoxicity against HeLa S3 cells with an  $IC_{50}$  value of 0.04  $\mu$ g/mL, and exhibited 50% growth inhibition against a panel of 39 human cancer cell lines with a  $GI_{50}$  value of 40 nM (Table 1). It exhibited strong protein kinase inhibition by phosphorylating extracellular signal-regulated protein kinase (ERK) in normal rat kidney (NRK) cells via platelet-derived growth factor (PDGF) stimulation at a 0.1–10  $\mu$ M concentration [20]. However, studies have shown that bisebromoamide and its synthetic analogs, whose stereochemistry reveals the presence of a methylthiazoline moiety and a methyl group at the 4-methylproline unit, do not significantly influence cytotoxicity against HeLa S3 cancer cells [21]. Bisebromoamide inhibited the phosphorylation of ERK and AKT (protein kinase) enzymes when tested against human renal carcinoma cell lines 769-P and 786-O. The  $IC_{50}$  values for 769-P and 786-O cells were 1.63  $\mu$ M and 2.11  $\mu$ M, respectively [22]. In another study, it was shown to induce apoptosis through ERK and mTOR inhibitions in renal cancer cells [23].

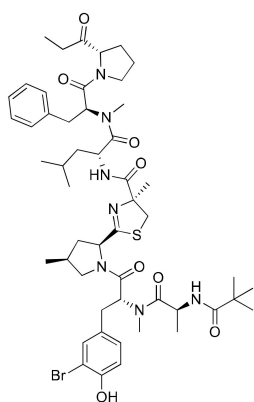


**Figure 5.** Chemical structure of bisebromoamide.

### 2.5. Biselyngbyaside

Biselyngbyaside A (Figure 6), a glycomacrolide isolated from *Lyngbya* sp., exhibits cytotoxicity against HeLa S3 cells with an  $IC_{50}$  value of 0.1  $\mu\text{g/mL}$  [24]. Moreover, Biselyngbyolide B, C, E and F have an antiproliferative effect in HeLa and HL-60 cells, and biselyngbyolide C was found to trigger endoplasmic reticulum (ER) stress and apoptosis in HeLa cells [25] (Table 1).

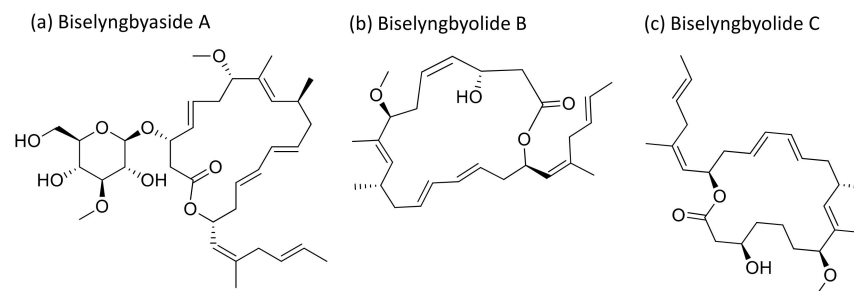


**Figure 6.** Chemical structure of biselyngbiasides.

### 2.6. Borophycin

Borophycin (boron-containing metabolite) is an acetate-derived polyketide (Figure 7) isolated from *Nostoc linckia* and *N. spongiaeforme* var. *tenuis*, which exhibits potent cytotoxicity against human colorectal adenocarcinoma (LoVo) and human cervical adenocarcinoma (KB) cell lines [26] (Table 1).

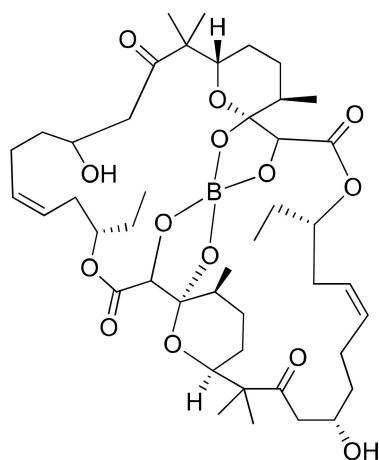


**Figure 7.** Chemical structure of borophycin.

### 2.7. Calothrixin

Calothrixins are quinone-based bioactive molecules (Figure 8) isolated from *Calothrix* that possess potent antiproliferative activity against several cancer cell lines [27]. Calothrixins A, an indolophenanthridine isolated from *Calothrix*, induced apoptosis and cell cycle arrest in the G2/M phase of several human cancer cell lines (Table 1). It has shown antitumor activity against human HeLa cancer cells at nanomolar concentrations [28]. Besides this, calothrixin B displayed antiproliferative activity against the HCT-116 colon cancer cell line with an  $IC_{50}$  value of 0.32  $\mu\text{M}$  [29]. Recently, a series of calothrixin B analogs have been synthesized that inhibit cancer cell growth by extensive DNA damage followed by apoptotic cell death. They have shown cytotoxicity against the NCI-H460 cell line with a  $GI_{50}$  of 1 nM [30]. Another analog of calothrixin B, isothiacalothrixin B, exhibits cytotoxicity against human colon cancer cells in vitro by inducing irreversible DNA damage, and causes apoptosis. It was found to be a promising anti-cancer agent that caused the strong arrest of the cells in the S and G2/ M phases of the cell cycle in the HCT116 cell line [31].

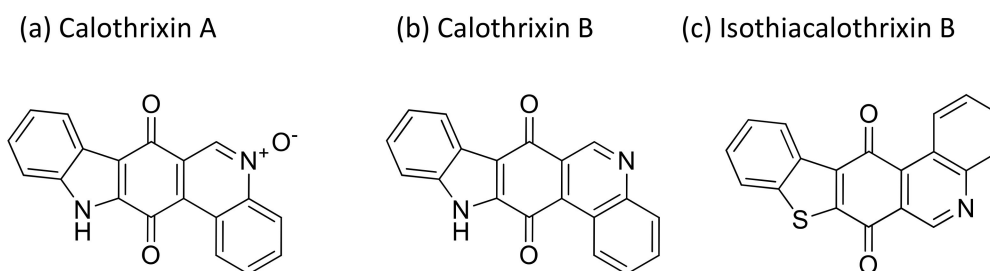


Figure 8. Chemical structure of calothrixins.

### 2.8. Carmaphycins

Carmaphycins A and B (Figure 9), isolated from *Symploca* sp., are structurally related to proteasome inhibitor epoxomicin, and show strong antiproteasomal activity. They exhibited strong cytotoxicity against lung adenocarcinoma (NCI-H460) and colon (HCT-116) cancer cell lines, as well as exquisite antiproliferative effects in the NCI-60 cell lines [32] (Table 1). Recently, carmaphycins conjugates with peptides and antibodies have been investigated in the design of novel antibody–drug conjugates (ADCs) for targeted delivery in cancer therapy [33].

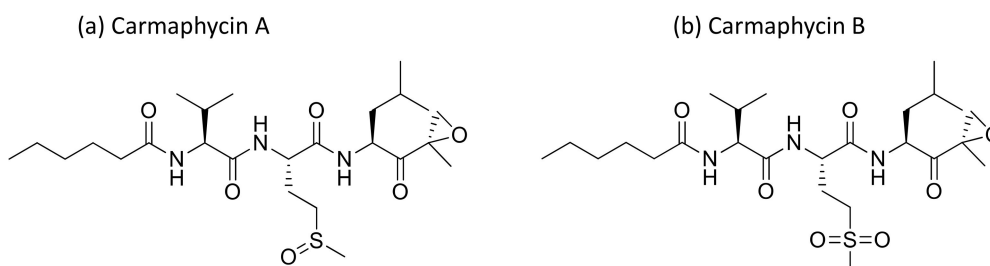


Figure 9. Chemical structure of carmaphycins.

### 2.9. Caylobolide

Caylobolide A and B are macrolactones (Figure 10) isolated from *Lyngbya majuscula* and *Phormidium* sp. that induce cytotoxicity against several cancer cell lines (Table 1). Caylobolide A exhibits cytotoxicity against the HCT-116 colon tumor with an  $IC_{50}$  of 9.9  $\mu$ M [34], while the  $IC_{50}$  values of Caylobolide B against the HT29 colorectal adenocarcinoma and HeLa cervical carcinoma are 4.5 and 12.2  $\mu$ M, respectively [35].

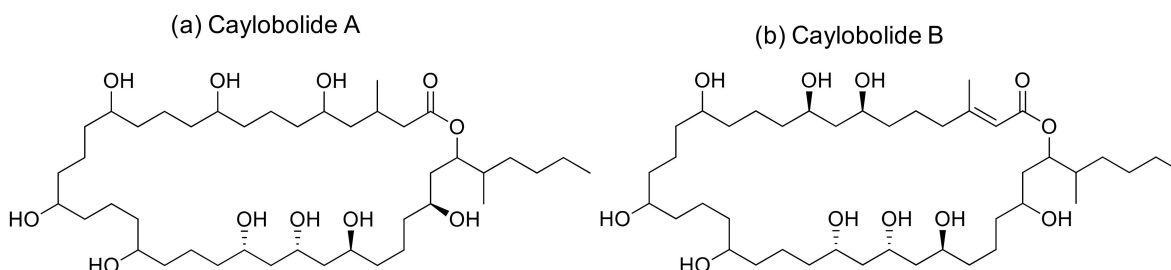
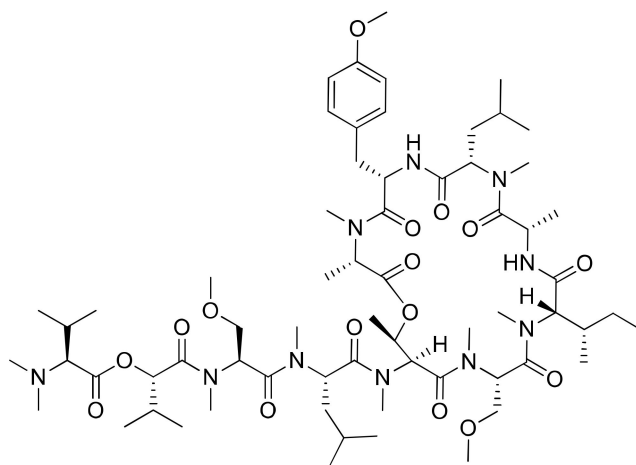


Figure 10. Chemical structure of caylobolides.

### 2.10. Coibamide A

Coibamide A (Figure 11) is a novel N-methyl-stabilized antiproliferative depsipeptide extracted from *Leptolyngbya* sp. that induces concentration- and time-dependent cytotoxicity with a half-maximal effective concentration ( $EC_{50}$ ) < 100 nM in human SF-295 and U87-MG glioblastoma cells and mouse embryonic fibroblasts (MEFs) (Table 1). It

induces mTOR-independent autophagy and cell death in human glioblastoma cells [36]. In addition, it displayed potent cytotoxicity towards the NCI-H460 lung cancer cells and mouse neuro-2a cells when used in nanomolar concentrations ( $LC_{50} < 23$  nM). Previously, it was evaluated against an in vitro panel of 60 selective human cancer cell lines, including colon, breast and ovarian malignant tumors cells. The results indicated that coibamide A was found to be more effective against the MDA-MB-231 breast cancer cell line than against other cell lines [37]. Recently, an analog of coibamide A was synthesized that significantly inhibited tumor growth in vivo [38].



**Figure 11.** Chemical structure of coibamide A.

### 2.11. Cryptophycins

Cryptophycin, a depsipeptide isolated from *Nostoc* sp. var. ATCC 53789 and GSV 224, is a potent anticancer agent. It inhibits microtubule assembly, and exhibited anti-tumorigenic activity against several solid tumors implanted in mice, including multidrug-resistant cancer cells (Table 1). The  $IC_{50}$  value was found to be less than 50 pM for multidrug-resistant cancer cell lines [39,40]. Several natural and synthetic analogs of cryptophycins (Figure 12) were reported and progressed to preclinical and clinical trials. Cryptophycin-8, a semi-synthetic analog, showed more efficient in vivo antiproliferative activity, leading it to act as an antitumor agent. Cryptophycin 52 (LY355703), isolated from *Nostoc* spp., induced cell cycle arrest in the G2/M phase and apoptosis via multiple pathways, such as both caspase-1- and caspase-3-dependent activation and Bcl-2 and Bcl-xL phosphorylation in several human prostate cancer cell lines [41]. A clinical phase II study of cryptophycin-52 revealed anticancer activity against advanced human non-small cell lung carcinoma (NSCLC) and platinum-resistant advanced ovarian cancer in patients [42], but failed due to neurotoxic side effects and limited in vivo efficacy [43]. Cryptophycins are promising drug candidates as their activity is not negatively affected by P-glycoprotein (a drug efflux system commonly found in multidrug-resistant tumor cell lines). Recently, cryptophycin conjugates with antibodies and peptides were developed for targeted drug delivery in cancer therapy [44]. The antiproliferative activities of RGD-cryptophycin and iso-DGR-cryptophycin conjugates were evaluated against human melanoma cells M21 and M21-L. They exhibit anticancer activity at nanomolar concentrations with different expression levels of integrin  $\alpha_v\beta_3$ . In another study, the cryptophycin conjugate (RGD-cryptophycin) showed antiproliferative effects against M21 and M21-L human melanoma cell lines at nanomolar concentrations [45].

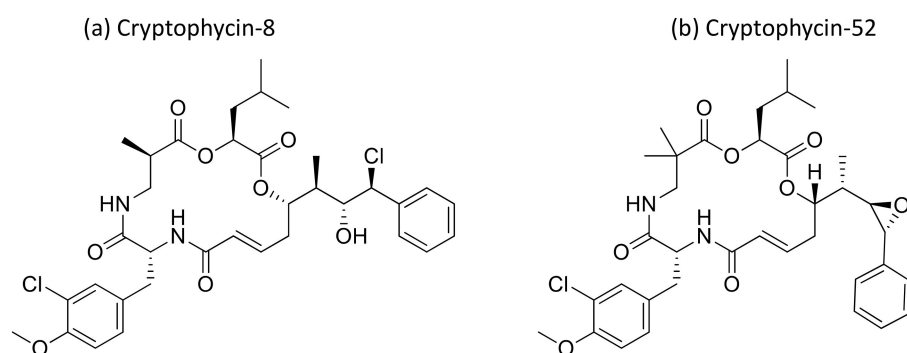


**Figure 12.** Chemical structure of cryptophycins.

### 2.12. Curacin A

Curacin A (Figure 13), an anti-tubulin agent isolated from *Lyngbya majuscula*, was screened against the NCI-60 panel of human tumor cell lines. It inhibits the binding of tubulin polymerization into the colchicine binding pocket, and arrests the cells in the G2/M phase of the cell cycle (Table 1). Due to its therapeutic potential as an antimitotic agent, curacin A was evaluated for clinical trials [46]. It exhibits cytotoxicity against renal, colon and breast cancer cell lines [47].

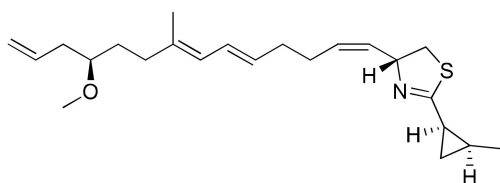


**Figure 13.** Chemical structure of curacin A.

### 2.13. Desmethoxymajusculamide C

Desmethoxymajusculamide C (Figure 14), a cyclic depsipeptide isolated from *L. majuscula*, exhibits strong antitumor potential against HCT-116 human colon carcinoma cells with an  $IC_{50}$  of 20 nM (Table 1). It helps in the destruction of the cell microfibrils networks by depolymerizing the actin cytoskeleton [48].

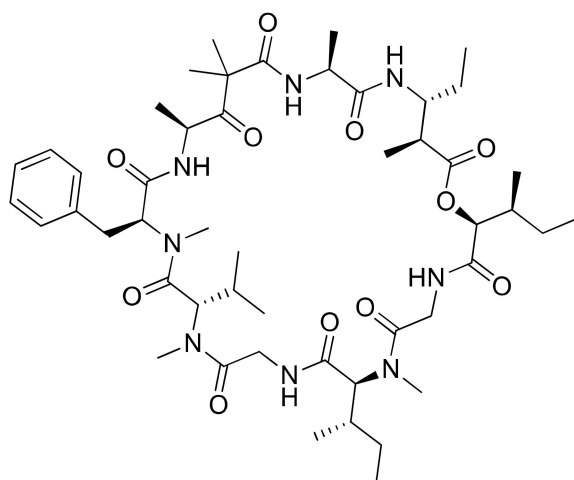


**Figure 14.** Chemical structure of desmethoxymajusculamide C.

### 2.14. Dolastatins

Dolastatins are peptides initially isolated from the sea hare *Dolabella auricularia* and later from marine cyanobacterial strains that induce cytotoxicity against cancer (Table 1). Dolastatins 10 and 15 (Figure 15a,b) are linear peptides isolated from a cyanobacteria,

*Symploca* sp. VP642 [49]. They show cytotoxicity against several cancer cell lines due to their specific molecular interference with the dynamics of microtubule assembly, and induce an arrest in the G2/M phase of the cell cycle, leading to apoptosis. Several synthetic and semi-synthetic analogs of dolastatins 10 and 15 have been produced and are in clinical trials as anticancer drugs. Symplostatin 3 (Figure 15c), a dolastatin analog isolated from *Symploca* sp. VP452, disrupts microtubules, and showed  $IC_{50}$  values ranging from 3.9 to 10.3 nM against KB and LoVo cell lines, respectively [50]. Dolastatin 10 and its synthetic analog auristatin PE underwent early clinical trial phases, but have been withdrawn owing to a lack of efficacy and reports of peripheral neuropathy in patients. Nevertheless, a highly effective antibody–drug conjugate (ADC) named brentuximab vedotin, developed by Seattle Genetics, passed the clinical trial and was granted FDA approval in August 2011 for the treatment of Hodgkin’s lymphoma and anaplastic large cell lymphoma. Brentuximab vedotin is a combination of monomethyl auristatin E, linked with an antibody targeting CD30 on cancer cell surfaces [51]. Additionally, three more dolastatin 10 analogs were formulated as antibody–drug conjugate ADCs, namely, glembatumumab vedotin, SGN75 and ASG5ME, which are in the clinical trials [52]. The cyanobacterial peptide named glembatumumab vedotin has been approved for Phase II trials. It exhibited potent activity against breast and melanoma cancers with the maximum tolerant doses of 1.0–1.88 mg/kg [53]. Furthermore, a new analog, auristatin TP (Figure 15d), has been synthesized, which is a tyramide phosphate modification of dolastatin 10. It possesses improved anticancer properties owing to its increased bioavailability, with  $ED_{50}$  values ranging from <1.2 to 54.6 nM when tested against P388, NCI-H460 and MCF-7 cancer cell lines [54]. Besides this, dolastatin-15 derivative-based ADCs have also been developed that effectively kill human epidermal growth factor receptor (HER)2-positive cancer cells [55]. Recently, using trastuzumab (Herceptin®) as the antibody, Dol10-containing ADCs have been synthesized and investigated for in vitro cytotoxicity assays against HER2-positive (SK-BR-3) human tumor cells. Additionally, ADCs derived from Herceptin® and PEG8-Dol10 effectively delayed tumor growth at a dose of 10 mg kg<sup>−1</sup>, and prolonged the survival time in mice bearing human ovarian SKOV-3 xenografts [56].

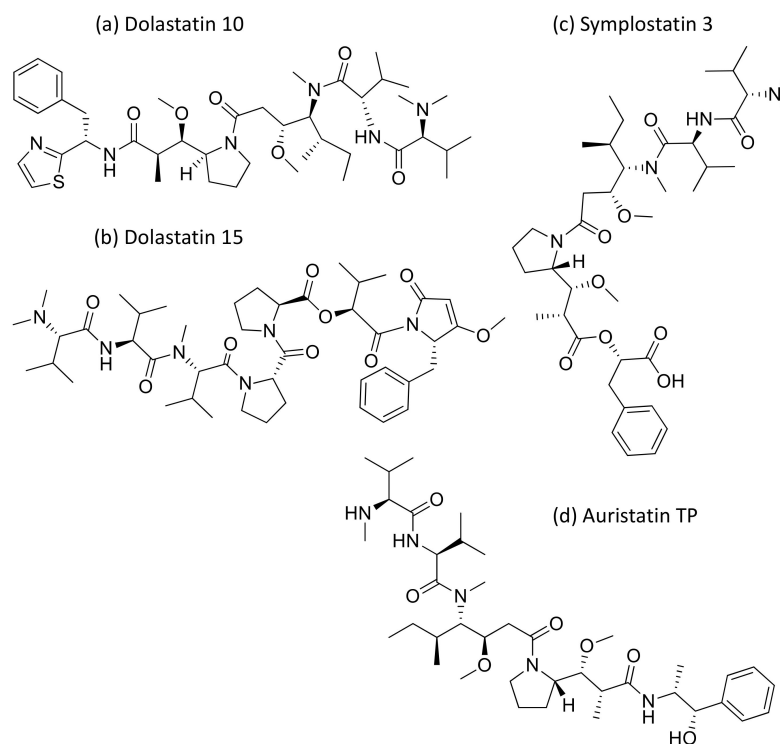


**Figure 15.** Chemical structure of some dolastatin analogs.



### 2.15. Grassypeptolides

Grassypeptolides A–C (Figure 16) are cyclic depsipeptides (containing bis-thiazoline) produced from *Lyngbya confervoides*, which reveal cytotoxicity against several cancer cells. The IC<sub>50</sub> values for grassypeptolides A were evaluated against HT29 and HeLa cancer cell lines, and were found to be 1.22 and 1.01  $\mu$ M, respectively (Table 1). Similarly, for grassypeptolides B and C, they were 4.97 and 2.93  $\mu$ M and 76.7 and 44.6 nM, respectively. Grassypeptolide A and C both induce G1 cell cycle arrest at lower concentrations, but in HeLa cells they induce the G2/M cell-cycle arrest at higher concentrations [57]. Furthermore, grassypeptolide D and E reveal cytotoxicity against HeLa cells at IC<sub>50</sub> values of 335 and 192 nM, respectively, and against mouse neuro-2a blastoma cells at IC<sub>50</sub> values of 599 and 407 nM, respectively [58].

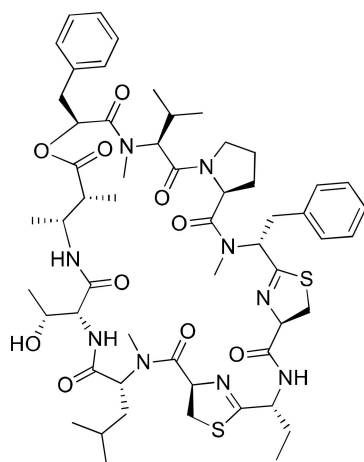


**Figure 16.** Chemical structure of grassypeptolide A.

### 2.16. Hantupeptin A

Hantupeptin A (Figure 17), a cyclodepsipeptide isolated from *L. majuscula*, exhibits cytotoxicity against the MOLT-4 leukemia and MCF-7 breast cancer cell line with IC<sub>50</sub> values ranging from 32 nM to 4.0  $\mu$ M, respectively [59] (Table 1).

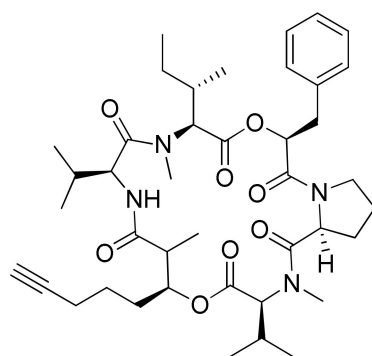


**Figure 17.** Chemical structure of hantupeptin A.

### 2.17. Hectochlorin

Hectochlorin (Figure 18) was isolated from *L. majuscula*, and promotes actin polymerization with an EC<sub>50</sub> value of 20  $\mu$ M in human non-tumoral kidney cells PtK2. It also displays cytotoxicity against the NCI-60 panel of cancer cell lines (Table 1). Among these, 23 cancer cell lines, such as colon melanoma, renal cells and ovarian cells, showed the strongest cytotoxicity. The IC<sub>50</sub> values range from 20 to 300 nM for CA46 human Burkitt lymphoma cell and PtK2 cells, respectively. However, the dose–response curve of hectochlorin was flat, suggesting that the compound is more antiproliferative than cytotoxic [60].

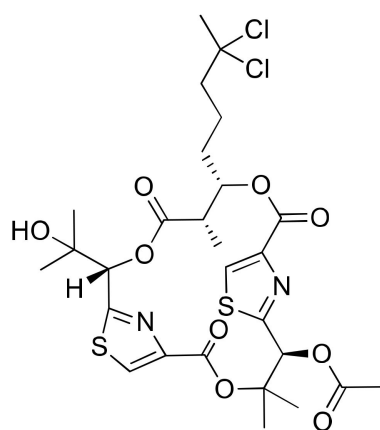


**Figure 18.** Chemical structure of hectochlorin.

#### 2.18. Hierridin B

Hierridin B (Figure 19), a polyketide isolated from the *Cyanobium* sp. LEGE 06113, was tested in a panel of eight human cancer cell lines, and showed selective cytotoxicity only against the colon adenocarcinoma cell line HT-29, with an  $IC_{50}$  value of 0.1 mM [60] (Table 1).

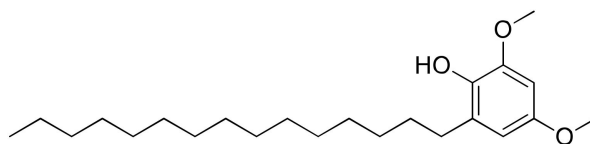


**Figure 19.** Chemical structure of hierridin B.

#### 2.19. Hoiamide D

Hoiamide D, isolated from *Symploca* sp, consists of a unique triheterocyclic system structurally comprising two consecutive thiazolines and a thiazole, as well as an unusual isoleucine moiety (Figure 20). The carboxylate anion of hoiamide D was reported to inhibit p53/HDM2 (human homolog of MDM2) interaction with an  $EC_{50}$  of 4.5 mM (Table 1). Besides this, it also possesses significant sodium channel-activating properties. [61].

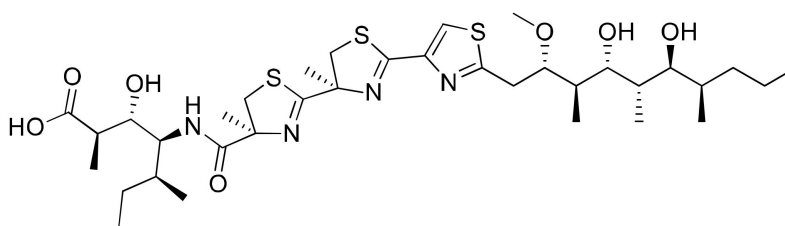


**Figure 20.** Chemical structure of hoiamide D.

#### 2.20. Hormothamnin A

Hormothamnin A (Figure 21), a cyclic undecapeptide (containing six common and five uncommon amino acid residues) isolated from *Hormothamnion enteromorphoides*, exhibits significant cytotoxicity against several solid cancer cell lines, such as human colon cells (HCT-116), human lung cells (SW1271 and A529) and murine melanoma cells (B16-F10), with  $IC_{50}$  values ranging from 0.13 to 0.72  $\mu\text{g/mL}$  [62] (Table 1).

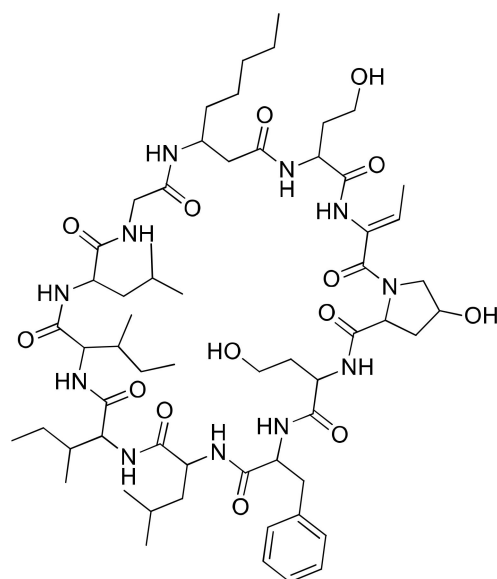


**Figure 21.** Chemical structure of hormothamnin A.

#### 2.21. Itralamides A and B

Itralamides A and B (Figure 22), cyclodepsipeptides isolated from *L. majuscula*, exhibit cytotoxicity against human embryonic kidney cells 293 (HEK293). Itralamide A showed lower cytotoxicity than Itralamide B against HEK293 cells with an  $IC_{50}$  of 6  $\mu M$  [40,63] (Table 1).

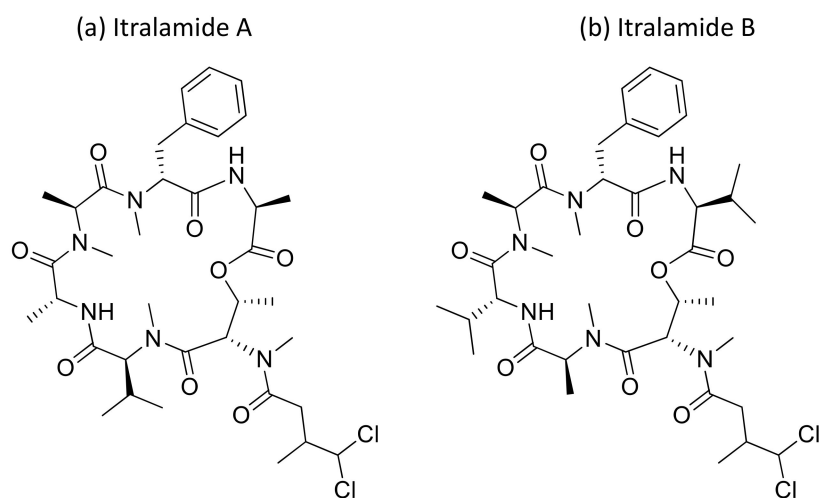


**Figure 22.** Chemical structure of itralamides A and B.

#### 2.22. Lagunamides

Lagunamide A (Figure 23a), isolated from *L. majuscula*, showed cytotoxicity against a panel of cancer cell lines, such as HCT8 (human colorectal cancer), P388 (murine leukemia), PC3 (human prostate cancer), A549 (human lung cancer) and SK-OV3 (human ovarian cancer), with  $IC_{50}$  values ranging from 1.6 nM to 6.4 nM (Table 1). The molecule exhibits an antiproliferative effect via mitochondria-mediated apoptosis against HCT8 and MCF7 (breast) cancer cell lines [64]. Furthermore, lagunamide A and B (Figure 23a,b) exhibit cytotoxicity against P388 murine leukemia cell lines with  $IC_{50}$  values of 6.4–20.5 nM, respectively [65]. In another study, Lagunamide C (Figure 23c) revealed strong cytotoxicity against A549, PC3, P388, HCT8, and SK-OV3 cell lines with  $IC_{50}$  values ranging from 2.1 to 24.4 nM [66]. In addition, Lagunamide A and D (Figure 23a,d) exhibited antiproliferative activity against A549 human lung adenocarcinoma cells with an  $IC_{50}$  value of 6.7–7.1 nM, respectively [67]. Recently, a molecular mechanism study in A549 human lung

adenocarcinoma cells showed that lagunamide-A induced caspase-mediated mitochondrial apoptosis [68].

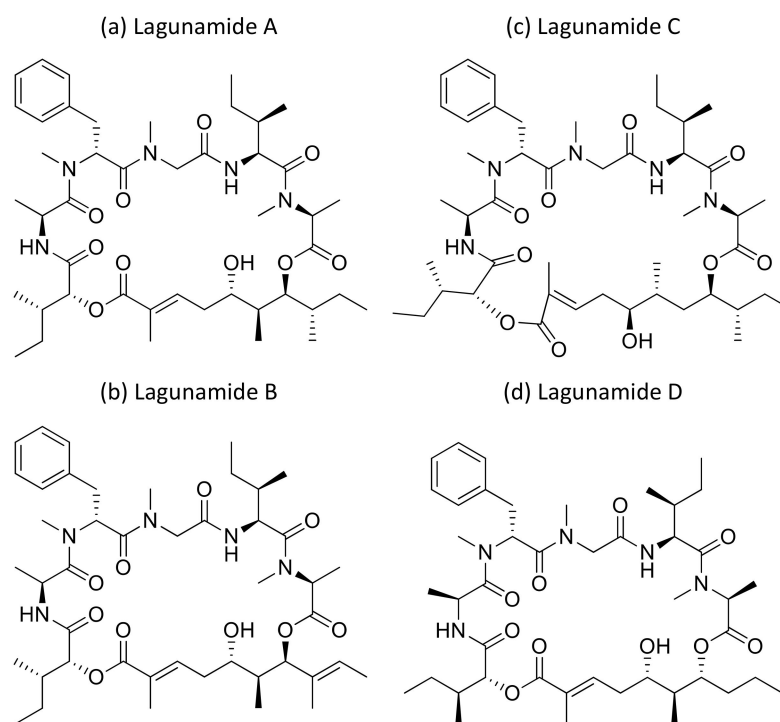


**Figure 23.** Chemical structure of lagunamides.

### 2.23. Largazole

Largazole (Figure 24), a cyclic depsipeptide isolated from *Symploca* sp., is a highly potent class I histone deacetylase (HDAC) inhibitor, and is currently being used for the development of anticancer drugs. It has been screened to evaluate its cytotoxicity against many epithelial and fibroblastic cancer cell lines [69] (Table 1). Generally, largazole acts as a prodrug, and upon hydrolysis of the thioester, a largazole thiol releases that function as a reactive molecule. The resultant molecule then complexes with  $\text{Zn}^{2+}$  and inhibits class I histone deacetylase. Beside its HDAC inhibitory property, largazole exhibits a wider range of in vitro and in vivo biological activities, for example antitumor, antiosteogenic and antifibrotic activities [70–72]. When largazole was used together with dexamethasone (a synthetic glucocorticoid steroid), it induced E-cadherin localization at the plasma membrane in triple-negative breast cancers and suppressed cancer invasion [73]. In another study, largazole sensitized Epstein–Barr virus-positive (EBV<sup>+</sup>) lymphoma cells to ganciclovir (an antiherpes viral drug) at nanomolar concentrations [74]. Recently, largazole and its analogs were found to inhibit a ubiquitin-activating enzyme (E1) during ubiquitination [75].

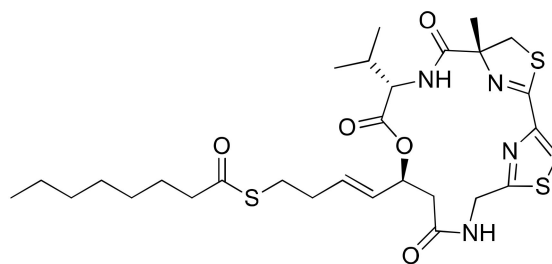


**Figure 24.** Chemical structure of largazole.

### 2.24. Laxaphycins

Laxaphycin A and B (Figure 25a,b) are cyclic peptides generally isolated from *Anabaena laxa*. Laxaphycin A showed weak cytotoxicity against certain cancer cell lines (Table 1) such as A549, MCF7, PA1 (ovarian teratocarcinoma), PC3, DLD1 (colorectal adenocarcinoma) and M4Beu (melanoma). However, laxaphycin B revealed strong anticancer activity against both resistant and sensitive cancer cell lines [76]. Recently, laxaphycins B4 and A2 (Figure 25c,d) were isolated from *H. enteromorphoides*, along with the known compound laxaphycin A. Laxaphycin B4 exhibited antiproliferation activity against human colon cancer HCT116 cell lines with an  $IC_{50}$  value of 1.7  $\mu$ M, whereas laxaphycins A and A2 revealed weak activities [77].

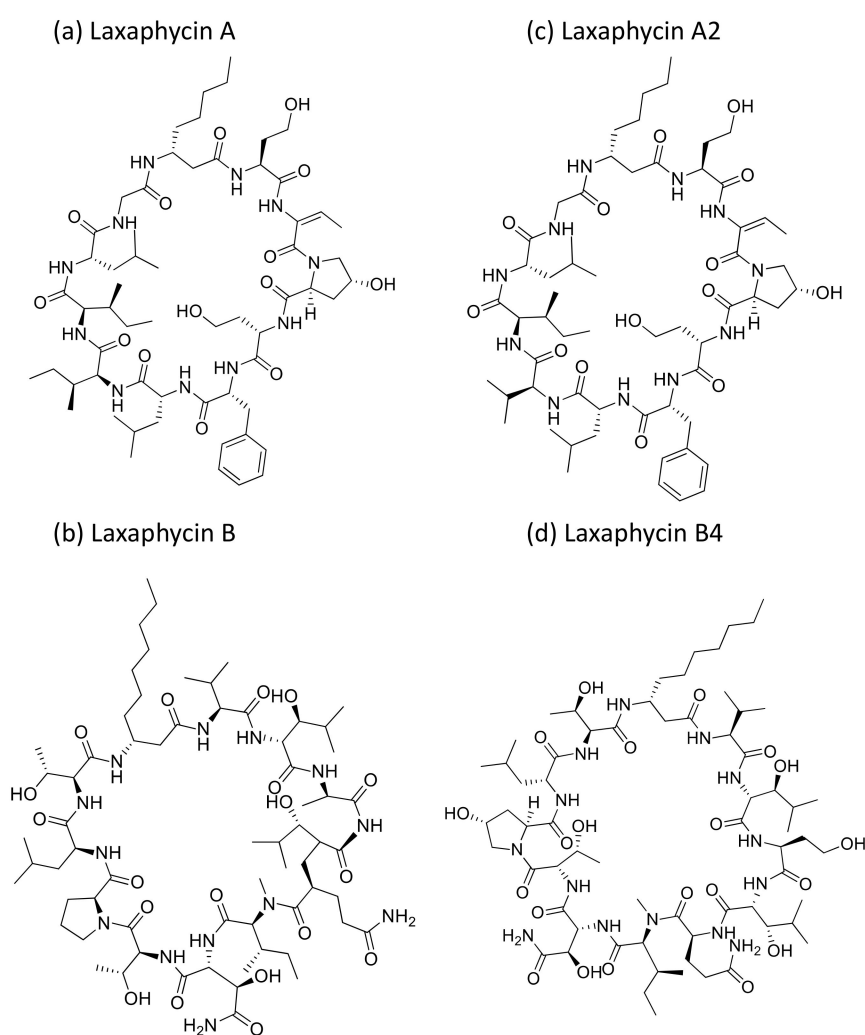


**Figure 25.** Chemical structure of laxaphycins.

### 2.25. Lyngbyabellins

Lyngbyabellin A and E (Figure 26a,b), isolated from *L. majuscula*, are hectochlorin-related lipopeptides. They possess potent actin polymerization activity. Lyngbyabellin A exhibited moderate cytotoxicity against human cervical (KB) and colon (LoVo) cancer cell lines with  $IC_{50}$  values of 0.03  $\mu$ g/mL and 0.5  $\mu$ g/mL, respectively (Table 1) [78]. In vivo trials suggested that lyngbyabellin A is toxic to mice. It disrupts the cellular microfilament network in A-10 cells at 0.01–5.0  $\mu$ g/mL concentrations [78]. When compared to the above, Lyngbyabellin B was found to be slightly more cytotoxic in in vitro trials [79]. Furthermore, Lyngbyabellin E showed cytotoxicity against human lung tumors (NCI-H460) and neuro-2a mouse neuroblastoma cell lines with  $LC_{50}$  values between 0.2 and 4.8  $\mu$ M [80].

Lyngbyabellin N (Figure 26f) exhibited strong cytotoxic activity against the HCT116 colon cancer cell line ( $IC_{50} = 40.9 \pm 3.3$  nM), while lyngbyabellins K, L, M and 7-epi-lyngbyabellin L (Figure 26c–e) do not show any activity [81].

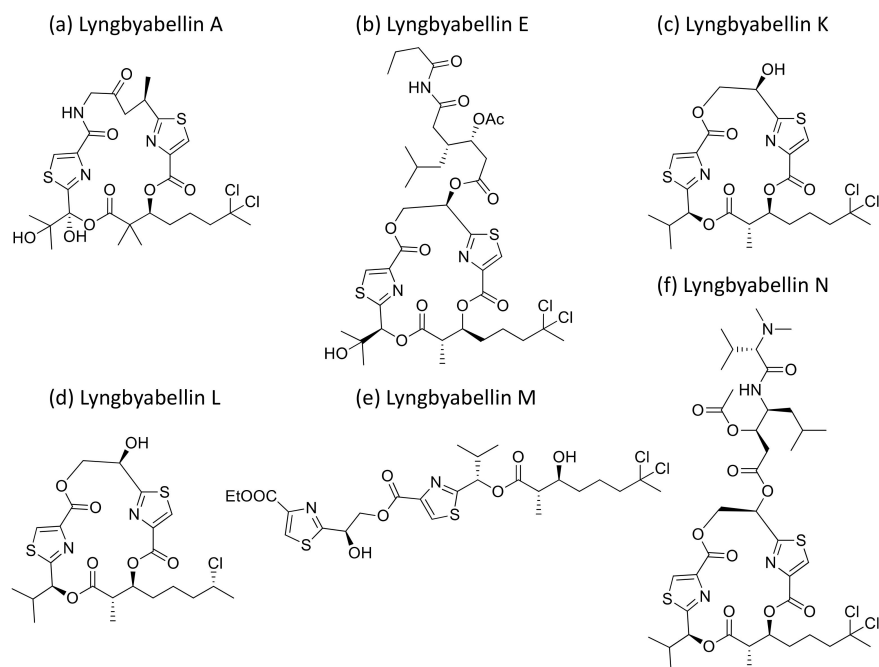


**Figure 26.** Chemical structure of lyngbyabellins.

## 2.26. Lyngbyastatins

Lyngbyastatins (Figure 27) are cyclic depsipeptides isolated from *Lyngbya* sp. that exhibit strong serine proteases inhibition. Lyngbyastatins 4 to 7 are potent inhibitors of elastase, with  $IC_{50}$  values ranging from 120 to 210 nM [82]. Furthermore, Lyngbyastatins 8–10, isolated from *Lyngbya semiplena*, inhibit porcine pancreatic elastase, with  $IC_{50}$  values ranging from 120 to 210 nM [83] (Table 1).

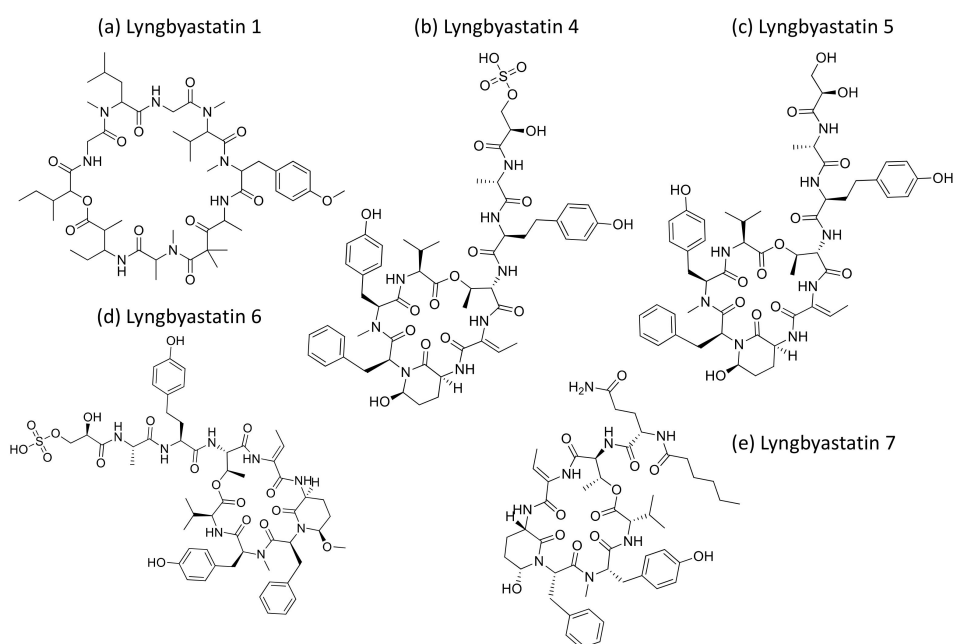


**Figure 27.** Chemical structure of lyngbyastatins.



### 2.27. Malyngamides

Malyngamides (Figure 28), small amides produced by *L. majuscula*, exhibit antiproliferative activity against tumor cells at the level of nanomolar to micromolar concentrations (Table 1). Isomalyngamides A and A-1, analogs of malyngamide, inhibit tumor proliferation by inactivating the expression and phosphorylation of FAK and Akt through the  $\beta$ 1 integrin-mediated antimetastatic pathway [84]. Another analog, malyngamide C and 8-epi-malyngamide C (Figure 28b), showed cytotoxicity against HT29 colon cancer cells with  $IC_{50}$  values of 5.2 and 15.4  $\mu$ M, respectively [85]. Additionally, Merocyclophanes A (Figure 28e) and B, isolated from *Nostoc* sp. (UIC 10022A), exhibited antiproliferative activity against the above cell lines with  $IC_{50}$  values of 3.3 and 1.7  $\mu$ M, respectively [86]. Recently, three new malyngamides were isolated from *Moorea producens* and, in particular, 6,8-di-O-acetylmalyngamide-2 showed strong anticancer activity by activating adenosine monophosphate-activated protein kinase (AMPK) [87].

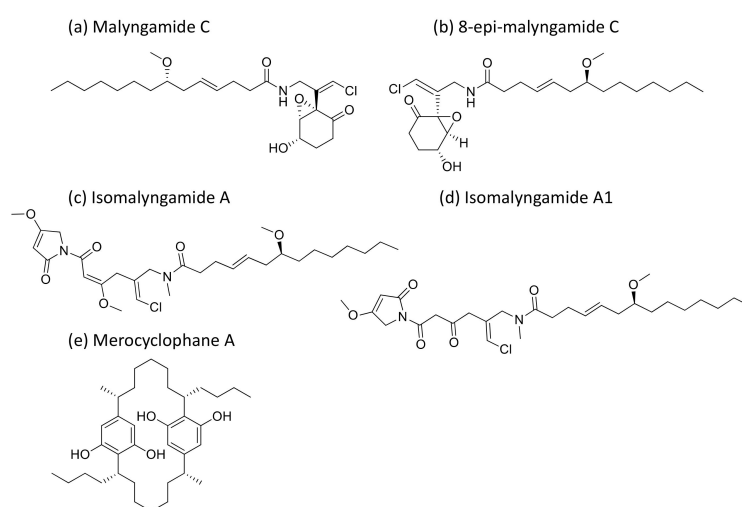


**Figure 28.** Chemical structure of malyngamides and derivatives.

### 2.28. Nocuolin A

Nocuolin A (Figure 29a), a natural oxadiazine isolated from some of the species belonging to *Nostoc*, *Nodularia* and *Anabaena* genera, induces cell death and exhibits anti-proliferative activity against various human cancer cells, specifically against p53-mutated cell lines with  $IC_{50}$  values ranging from 0.7 to 4.5  $\mu$ M [88] (Table 1).

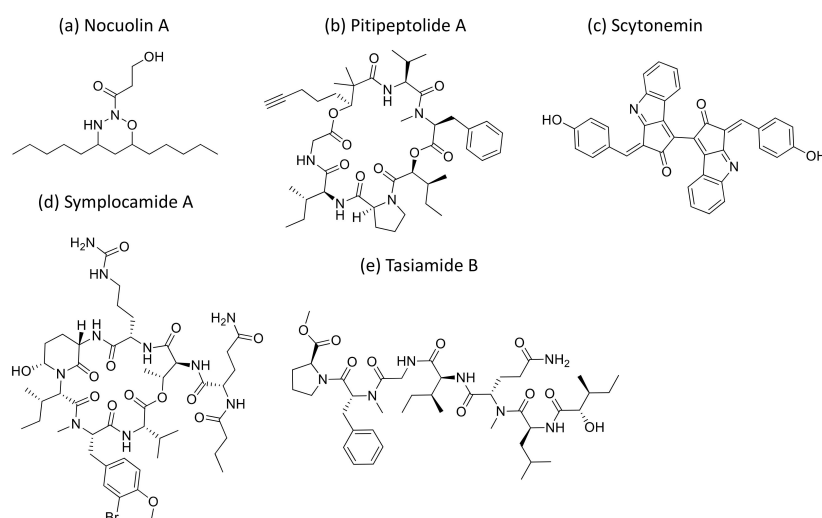


**Figure 29.** Chemical structure of nocuolin A (a), pitipeptolide A (b), scytonemin (c), symplocamide A (d) and Tasiamide (e).

### 2.29. Pitipeptolides

Pitipeptolides (Figure 29b) are cyclic depsipeptides isolated from *L. majuscula*. Pitipeptolides A, B, and C–F revealed cytotoxicity against HT 29 colon adenocarcinoma and MCF-7 breast cancer cell lines, with an  $IC_{50}$  value between 10 and 100  $\mu$ M [89] (Table 1).

### 2.30. Scytonemin

Scytonemin (Figure 29c), an aromatic indole alkaloid extracted from *Stigonema* sp., showed antiproliferative activity against several human fibroblast and endothelial cell lines. It inhibits the human polo-like kinase activity that plays a crucial role in the regulation of the cell cycle at the G2/M transition [90] (Table 1).

### 2.31. Symplocamide A

Symplocamide A (Figure 29d), a cyclodepsipeptide isolated from *Symploca* sp., showed potent cytotoxicity against non-small cell lung cancer cells NCI-H460 ( $IC_{50}$  = 40 nM) and neuro-2a neuroblastoma cells ( $IC_{50}$  = 29 nM) by inhibiting serine proteases activity ( $IC_{50}$  = 0.38  $\mu$ M) [91] (Table 1).

### 2.32. Tasiamides

Tasiamides are linear peptides isolated from *Symploca* sp. and tasiamide B (Figure 29e) that showed strong cytotoxicity against human cervical adenocarcinoma (KB) cells, with an  $IC_{50}$  value of 0.8  $\mu$ M [92]. In another study, eighteen analogs of tasiamide were screened against KB cells and human non-small cell lung tumor A549 cells, with  $IC_{50}$  values between 1.29 and 12.88  $\mu$ M, respectively [93] (Table 1).

### 2.33. Veraguamides

Veraguamides A–C and H–L cyclodepsipeptides (Figure 30) were isolated from *Oscillatoria margaritifera*, and veraguamides A–G were also isolated from *Symploca hydroides*. All showed a cytotoxic effect (Table 1). Veraguamide A was found to be highly toxic against the human lung cancer cell line NCI-H460 ( $LD_{50}$  = 141 nM) [94]. Moreover, veraguamides A–G exhibited moderate to weak cytotoxicity against both the HT 29 and HeLa cell lines [95].

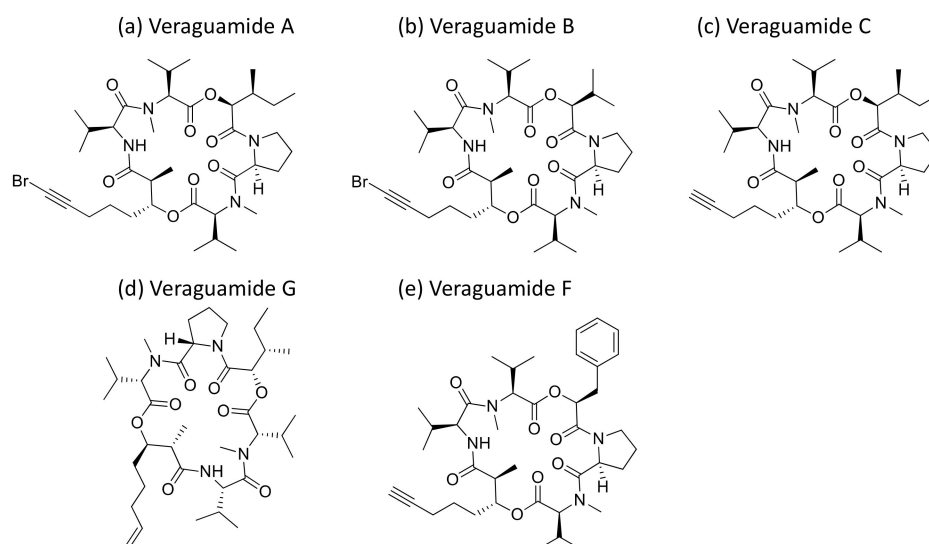


**Figure 30.** Chemical structure of veraguamides.

### 2.34. Miscellaneous

Kempopeptins A and B (cyclodepsipeptides from *Lyngbya* sp.), Bouillomides A and B (depsipeptides from *Lyngbya bouillonii*), Molassamide (depsipeptide from *Dichothrixutahensis*), Largamides (cyclic peptides from *Lyngbya confervoides*), Pompanopeptin A, (cyclic peptide from *L. confervoides*), and all dolastatin 13 analogs, strongly inhibit non-caspase

proteases' activity with  $IC_{50}$  values ranging from 0.32 to 25.0  $\mu M$  [4]. Kempopeptin C has recently been isolated as a serine protease inhibitor. It is a chlorinated analog of kempopeptin B that inhibited the migration of invasive breast cancer (MDA-MB-231) cells by 37–60% at the 10 and 20  $\mu M$  concentrations [96]. Furthermore, Belamide A (Figure 31a), a linear tetrapeptide isolated from *Symploca* sp., exhibits cytotoxicity against HCT-116 colon cancer with an  $IC_{50}$  of 0.74  $\mu M$  by disturbing microtubule formation [97] (Table 1).

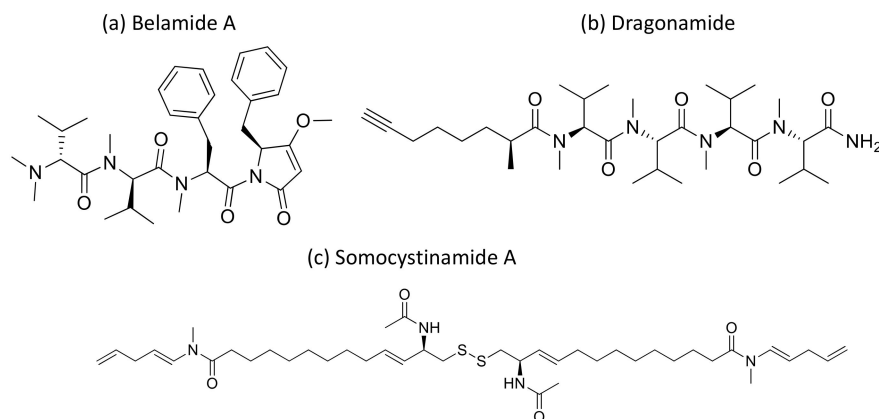


**Figure 31.** Chemical structure of belamide A (a), dragonamide (b) and somocystinamide A (c).

Moreover, dragonamide (Figure 31b), a lipopeptide isolated from *L. majuscula*, induces cytotoxicity on P-388, A-549, HT-29 and MEL-28 cancer cells with an  $IC_{50} > 1 \mu g/mL$  [98] (Table 1). Recently, a cyanobacterial species named *Fischerella* has been isolated from the Nile river. The different compounds isolated from it have been explored and were found to be active against breast cancer (MCF-7), liver cancer (HepG-2), colon cancer (HCT116), and lung cancer (A549) cell lines. However, its crude extract BS1-EG exhibited various effects on all tested cell lines [99].

Malevamide D and E (Figure 32) are peptide esters isolated from *S. hydroides* that induce cytotoxicity against P-388, A-549, HT-29, and SK-MEL-28 (human melanoma) cell lines with  $IC_{50}$  values ranging from 0.3 to 0.7 nM [100] (Table 1). Somocystinamide A (Figure 31c), a lipopeptide isolated from *L. majuscula*, exhibits cytotoxicity on Jurkat ( $IC_{50}$  3 nM) and CEM leukemia ( $IC_{50}$  14 nM), A549 lung carcinoma ( $IC_{50}$  46 nM), Molt4 T leukemia ( $IC_{50}$  60 nM), M21 melanoma ( $IC_{50}$  1.3 nM) and U266 myeloma ( $IC_{50}$  5.8  $\mu M$ ) cell lines by inducing apoptosis via caspase 8 [101] (Table 1). Tiglicamides A–C (Figure 33a–c), Ulongapeptin (Figure 33d) and Obyanamide (Figure 33e), which are cyclic depsipeptides isolated from *Lyngbya* sp., induce cytotoxicity in cancer cell lines, such as KB cells, with  $IC_{50}$  values ranging from 2.14 to 7.28  $\mu M$ , 0.63  $\mu M$  and 0.58  $\mu g/mL$ , respectively, and later inhibit the serine proteases pathway [102–104] (Table 1). Wewakpeptins, a depsipeptide from *L. semiplena*, showed anticancerous potential against NCI-H460 lung cancer with an  $LD_{50}$  of 0.4  $\mu M$  [105] (Table 1).

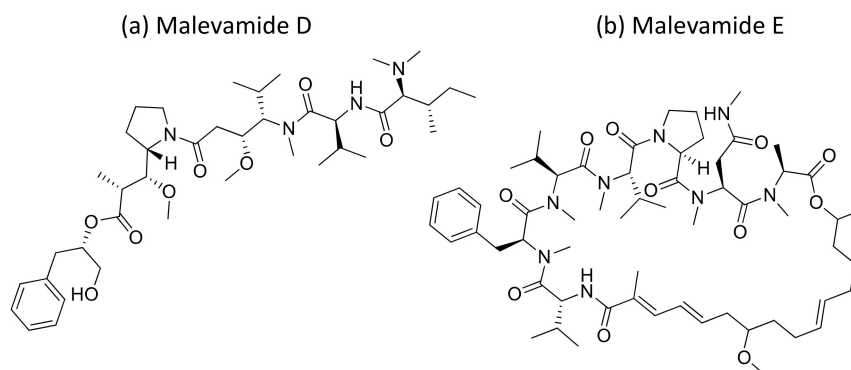


**Figure 32.** Chemical structure of mavelamide D and E.

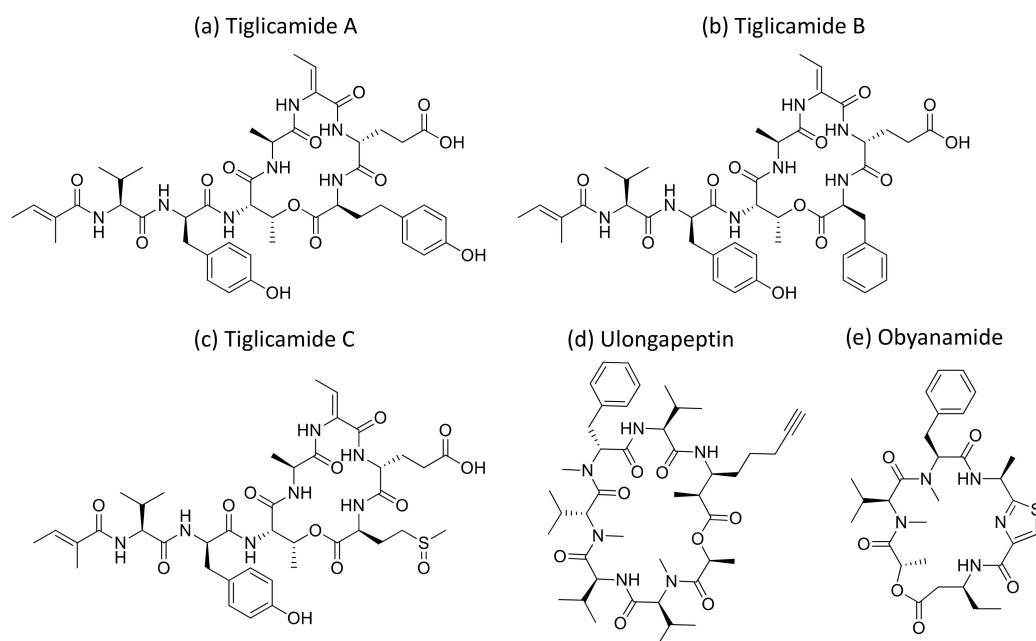


**Figure 33.** Chemical structure of tiglicamide A to C (a–c), ulongapeptin (d) and oby NAMide (e).

Moreover, the cyclic depsipeptide Homodolastatin 16 (Figure 34a) [106], the polyketide-peptides Jamaicamide A–C (Figure 35) [107], and the cyclodepside malyngolide dimer (Figure 34b) [108], all isolated from *L. majuscula*, induce cytotoxicity against several human tumor cells such as the oesophageal WHCO1 and WHCO6, cervical ME180, breast MCF-7 and MDA-MB-231, and lung NCI-H460 cancer cell lines (Table 1). Recent evidence has shown the antiproliferative activity of the depsipeptides anaenamide A and B extracted from Guam cyanobacteria [109]. Finally, Tutuilamides A–C, which are vinyl-chloride-containing cyclodepsipeptides identified from cyanobacterial field collections from American Samoa and Palmyra Atoll, display potent elastase inhibitory activity, together with moderate antiproliferative activity toward H-460 lung cancer cells [110].

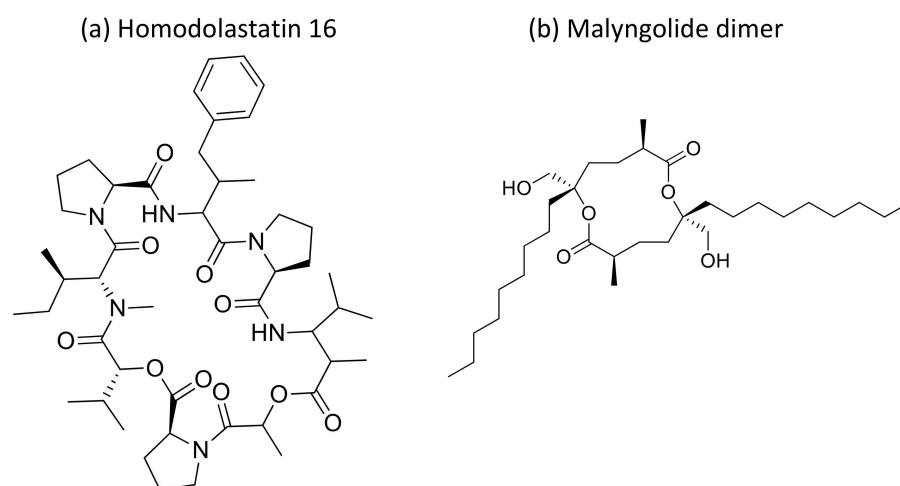


**Figure 34.** Chemical structure of homodolastatin 16 (a) and malyngolide dimer (b).

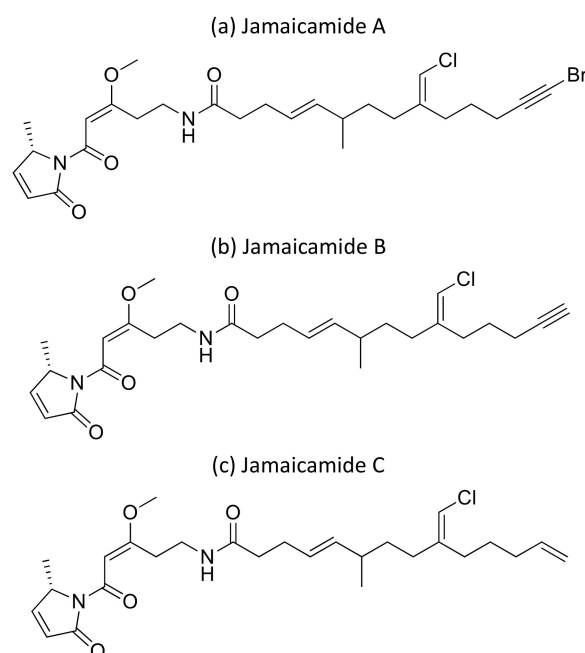


**Figure 35.** Chemical structure of jamaicamides.

**Table 1.** Summarized data of cyanobacterial secondary metabolites with anti-cancerous potential.

Compound Name	Analogs	Specific Class/Type	Source	In Vitro/In Vivo Cancer Cell Lines Screened	IC <sub>50</sub> /LC <sub>50</sub> /ED <sub>50</sub> /GI <sub>50</sub> Values	Molecular Targets	References
Ankaraolide A		Glycosylated swinholide	<i>Geitlerinema</i>	NCI-H460; MDA-MB-435	IC <sub>50</sub> = 119 nM IC <sub>50</sub> = 8.9 nM	Loss of filamentous actin	[8]
Apratoxin	Apratoxin A Apratoxin B-D Apratoxins A and E hybrid Oxazoline Apratoxin S10	Cyclic depsipeptide	<i>Lyngbya</i> sp.	LoVo, KB; HT29, HeLa, U2OS; NCI-H460	IC <sub>50</sub> = 0.36 nM IC <sub>50</sub> = 0.52 nM  IC <sub>50</sub> = 2.6 nM	Cell cycle arrest, apoptosis, secretory pathway inhibition	[9–16]
Aurilide	Aurilide B Aurilide C	Cyclic depsipeptide	<i>Dolabellaauriculari</i> and <i>Lyngbya majuscula</i>	NCI-H460, Neuro2a ; NCI-60 panel	LC <sub>50</sub> = 0.01 to 0.13 $\mu$ M GI <sub>50</sub> <10 nM	Mitochondrial induced apoptosis	[17]
Belamide A		Linear tetrapeptide	<i>Symploca</i> sp	HCT-116	IC <sub>50</sub> = 0.74 $\mu$ M	Microtubule disruption	[97]
Bisbromoamide		Peptide	<i>Lyngbya</i> sp	HeLa S3; 769-P; 786-O;	IC <sub>50</sub> = 0.04 $\mu$ g/mL IC <sub>50</sub> = 1.63 $\mu$ M IC <sub>50</sub> = 2.11 $\mu$ M	Actin filaments stabilization, protein kinase inhibition, induces apoptosis through ERK and mTOR inhibitions	[19–23]
Biselyngbyaside	Biselyngbyaside A Biselyngbyolide B, C, E	Glicomacrolide	<i>Lyngbya</i> sp.	HeLa S3, HeLa, HL-60	IC <sub>50</sub> = 0.1 $\mu$ g/ml	Induces ER stress and apoptosis	[24,25]
Borophycin			<i>Nostoc linckia</i> , <i>N. spongiaforme</i>	LoVo, KB			[26]
Calothrixin A	Calothrixin A Calothrixin B Isothiacalothrixin B	Pentacyclic indolophenanthridine	<i>Calothrix</i>	HeLa, HCT-116; NCI-H460	IC <sub>50</sub> = 0.32 $\mu$ M; GI <sub>50</sub> = 1 nM	Induced apoptosis and cell cycle arrest in S and G <sub>2</sub> /M phase	[27–31]
Carmaphycin	Carmaphycins A and B		<i>Symploca</i> sp.	NCI-H460, HCT-116		Proteasome inhibitor	[32]
Caylobolide	Caylobolide A and B	Macrolactone	<i>Lyngbya majuscula</i> , <i>Phormidium</i> spp	HCT-116; HT29; HeLa	IC <sub>50</sub> = 9.9 $\mu$ M IC <sub>50</sub> = 4.5 $\mu$ M IC <sub>50</sub> = 12.2 $\mu$ M		[34,35]
Coibamide A		Cyclic depsipeptide	<i>Leptolyngbya</i> sp.	SF-295, U87-MG, MEFs; NCI-H460, neuro-2a, MDA-MB-231	EC <sub>50</sub> < 100 nM  LC <sub>50</sub> < 23 nM	Induces mTOR-independent autophagy and cell death	[36,37]
Cryptophycin	Cryptophycin-8 Cryptophycin 52 (LY355703) RGD-cryptophycin and isoDGR-cryptophycin conjugates	Cyclic depsipeptide	<i>Nostoc</i> sp. var. ATCC 53789 and GSV 224	NSCLC, multidrug-resistant cancer cell lines (M21, M21-L), platinum-resistant advanced ovarian cancer	IC <sub>50</sub> > 50 pM	Inhibits microtubule assembly, induces cell cycle arrest in G <sub>2</sub> /M phase and apoptosis	[39–42]
Curacin A		Lipopeptide	<i>Lyngbya majuscula</i>	NCI-60 panel		Tubulin polymerization inhibition, cell cycle arrest at G <sub>2</sub> /M phase	[46,47]

Table 1. Cont.

Compound Name	Analogs	Specific Class/Type	Source	In Vitro/In Vivo Cancer Cell Lines Screened	IC <sub>50</sub> /LC <sub>50</sub> /ED <sub>50</sub> /GI <sub>50</sub> Values	Molecular Targets	References
Desmethoxymajusculamide C		Cyclic depsipeptide	<i>L. majuscula</i>	HCT-116	IC <sub>50</sub> = 20 nM	Destroys cell microfilaments networks	[48]
Dolastatins	Dolastatins 10 Dolastatins 15  Symprostatin 3  Auristatin TP	Linear Pentapeptide	<i>Dolabella auricularia</i> <i>Symploca</i> sp. VP642 <i>Symploca</i> sp. VP452	KB, LoVo;  P388, NCI-H460, MCF-7,	IC <sub>50</sub> = 3.9 nM IC <sub>50</sub> = 10.3 nM  ED <sub>50</sub> < 1.2 to 54.6 nM	Interferes with the dynamics of microtubule assembly and induces an arrest in the G <sub>2</sub> /M phase of the cell cycle, leading to apoptosis	[49,50,54]
Dragonamide		Lipopeptide	<i>Lyngbya majuscula</i>	P-388, A-549, HT-29, MEL-28	IC <sub>50</sub> > 1 µg/ml		[98]
Grassystatins	Grassypeptolides A-E	Cyclic depsipeptides	<i>Lyngbya confervoides</i>	HT29; HeLa; neuro-2a	IC <sub>50</sub> = 76.7 nM to 4.97 µM IC <sub>50</sub> = 44.6 nM to 2.93 µM; IC <sub>50</sub> = 0.41 to 0.60 µM	Induces G <sub>1</sub> and G <sub>2</sub> /M phase cell cycle arrest	[57,58]
Hantupeptin A		Cyclodepsipeptide	<i>Lyngbya majuscula</i>	MOLT-4; MCF-7	IC <sub>50</sub> = 32 µM IC <sub>50</sub> = 4.0 µM		[59]
Hectochlorin		Lipopeptide	<i>Lyngbya majuscula</i>	CA46, PtK2; NCI-60 panel	IC <sub>50</sub> = 20 nM IC <sub>50</sub> = 0.3 µM GI <sub>50</sub> = 5.1 µM	Cell cycle inhibition by promoting actin polymerization	[60]
Hierridin B		Polyketide	<i>Cyanobium</i> sp.	HT-29	IC <sub>50</sub> = 0.1 mM		[61]
Hoiamide	Hoiamide D	Cyclic depsipeptide	<i>Symploca</i> sp.		EC <sub>50</sub> = 4.5 mM	Inhibits p53/HDM2 and activates sodium-channels	[62]
Homodolastatin 16		Cyclic depsipeptide	<i>Lyngbya majuscula</i>	WHCO1; WHCO6; ME180	IC <sub>50</sub> = 4.3 µg/mL IC <sub>50</sub> = 10.1 µg/mL; IC <sub>50</sub> = 8.3 µg/mL		[106]
Hormothamnion A		Cyclic undecapeptide	<i>Hormothamnion enteromorphoides</i>	HCT-116, SW1271, A529, B16-F10	IC <sub>50</sub> = 0.13 to 0.72 µg/ml		[40]
Itralamide	Itralamide A and B	Cyclodepsipeptides	<i>L. majuscula</i>	HEK293	IC <sub>50</sub> = 6 µM		[63]
Jamaicamides A–C		Polyketide-Peptides	<i>Lyngbya majuscula</i>	NCI-H460	LC <sub>50</sub> = 15 µM		[107]
Lagunamide	Lagunamides A Lagunamides B Lagunamide C Lagunamide D	Cyclic depsipeptide	<i>Lyngbya majuscula</i>	HCT8, P388, PC3, SK-OV3, MCF7; A549	IC <sub>50</sub> = 1.6 nM to 24.4 nM;  6.7 to 7.1 nM	Caspase-mediated mitochondrial apoptosis	[64–68]
Largazole		Cyclic depsipeptide	<i>Symploca</i> sp.	Epithelial and fibroblastic cancer cell lines		Inhibit class I histone deacetylase	[69]
Laxaphycin	Laxaphycin A and B Laxaphycins B4 and A2	Cyclic peptides	<i>Anabaena laxa</i> . <i>Hormothamnion enteromorphoides</i>	HCT-116; A549, MCF7, PA1, PC3, DLD1, M4Beu,	IC <sub>50</sub> = 1.7 µM		[76,77]
Lyngbyabellin	Lyngbyabellin A and E Lyngbyabellin K-N	Cyclic depsipeptide	<i>L. majuscula</i>	KB, LoVo; HCT116; NCI-H460, neuro-2a	IC <sub>50</sub> = 0.03 µg/mL IC <sub>50</sub> = 0.5 µg/mL; IC <sub>50</sub> = 40.9 nM LC <sub>50</sub> = 0.2 to 4.8 µM	Possesses actin polymerization activity, disrupts the cellular microfilament network	[78–81]
Lyngbyastatin	Lyngbyastatins 1 Lyngbyastatins 4–7	Cyclic depsipeptide	<i>Lyngbya majuscula</i> <i>Lyngbya semiplena</i>	None: in vitro enzyme assay	IC <sub>50</sub> = 120 to 210 nM	Inhibits serine proteases (elastase)	[82,83]
Malevamide	Malevamide D Malevamide E	Peptide ester	<i>Symploca hydroides</i>	P-388, A-549, HT-29, MEL-28	IC <sub>50</sub> = 0.3 to 0.7 nM		[100]
Malyngamide	Isomalyngamides A and A-1 malyngamide C and 8-epi-malyngamide C Merocyclophanes A and B 6,8-di-O-acetylmalyngamide 2 Malyngamide C, J and K	Fatty acid amine	<i>Lyngbya</i> sp.  <i>Nostoc</i> sp. (UIC 10022A), <i>Moorea producens</i>	MCF-7, MDA-MB-231  HT29	IC <sub>50</sub> = 4.6 µM IC <sub>50</sub> = 2.8 µM  IC <sub>50</sub> = 1.7 to 15.4 µM	Inactivates the expression of p-FAK, FAK, p-Akt and Akt through β1 integrin-mediated antitumorigenic pathway and activates AMPK	[84–87]
Malyngolide dimer		Cyclodepside	<i>Lyngbya majuscula</i>	NCI-H460	IC <sub>50</sub> = 19 µM		[108]
Noculin A (NoA)		Oxadiazine	<i>Nostoc</i> , <i>Nodularia</i> and <i>Anabaena</i>	p53 mutated cell lines	IC <sub>50</sub> = 0.7 to 4.5 µM	Induces cell death and exhibits anti-proliferative activity	[88]
Obyanamide		Cyclic depsipeptide	<i>Lyngbya confervoides</i>	KB	IC <sub>50</sub> = 0.58 µg/ml		[104]
Pitipeptolides	Pitipeptolides A-B and C-F	Cyclic depsipeptides	<i>Lyngbya majuscula</i>	HT 29, MCF-7	IC <sub>50</sub> = 10 to 100 µM		[89]
Scytonemin		Polysaccharide	<i>Stigonema</i> sp	Human fibroblast and endothelial cell lines		Inhibits human polo-like kinase activity that plays a crucial role in the regulation of the cell cycle at the G <sub>2</sub> /M transition	[90]



Table 1. Cont.

Compound Name	Analogs	Specific Class/Type	Source	In Vitro/In Vivo Cancer Cell Lines Screened	IC <sub>50</sub> /LC <sub>50</sub> /ED <sub>50</sub> /GI <sub>50</sub> Values	Molecular Targets	References
Somocystinamide A		Lipopeptide	<i>Lyngbya majuscula</i>	Jurkat; CEM; A549; Molt4 T; M21; U266	IC <sub>50</sub> = 3 nM IC <sub>50</sub> = 14 nM IC <sub>50</sub> = 46 nM IC <sub>50</sub> = 60 nM IC <sub>50</sub> = 1.3 µM IC <sub>50</sub> = 5.8 µM	Induces apoptosis selectively via Caspase 8	[79,101]
Symplocamide	Symplocamide A	Cyclodepsipeptide	<i>Symploca</i> sp.	NCI-H460; neuro-2a	IC <sub>50</sub> = 40 nM IC <sub>50</sub> = 29 nM	Serine proteases inhibitor	[91]
Tasiamide	Several analogs	Linear peptides	<i>Symploca</i> sp.	KB; A549	IC <sub>50</sub> = 0.8 to 8.5 µM IC <sub>50</sub> = 2.24 to 12.88 µM		[92,93]
Tiglicamides A–C		Cyclic depsipeptides	<i>Lyngbya confervoides</i>	None: in vitro enzyme assay	IC <sub>50</sub> = 2.14 to 7.28 µM	Serine protease inhibition (elastase)	[102]
Ulongapeptin		Cyclic depsipeptide	<i>Lyngbya</i> sp.	KB	IC <sub>50</sub> = 0.63 µM.		[103]
Veraguamides	Veraguamides A–C and H–L veraguamides A–G	Cyclic depsipeptides	<i>Oscillatoria margaritifera</i> <i>Symploca</i> cf. <i>hydroides</i>	NCI-H460; HT 29, HeLa	LD <sub>50</sub> = 141 nM		[94,95]
Wewakpeptins		Depsipeptides	<i>Lyngbya semiplena</i>	NCI-H460	LD <sub>50</sub> = 0.4 µM		[105]

### 3. Cyanobacteria as Nanoformulations in Cancer Therapies

Globally, the use of nanomaterials in the biomedical field has attracted the increasing interest of researchers because of their unique ability to interact with cells and tissues at the molecular level with a high degree of specificity and improved efficacy. The small size (ranging from 1 to 100 nm), design flexibility and large surface-to-volume ratio make these materials of significant use. With the appreciation of the enhanced properties of metals at nanosizes, extensive research on different nanometals has been carried out in recent years for exploring their applications in cancer research. Emphasizing the biological synthesis, cyanobacteria are considered as one of the best biological systems for nanoparticle (NP) synthesis, both intra-cellularly as well as extra-cellularly [111]. However, there are only a few reports available on the biological synthesis of noble metal NPs utilizing cyanobacteria as the host system. Silver (Ag) is the most commonly reported NP synthesized [111–113]. Besides this, gold (Au), palladium (Pd) and platinum (Pt) NPs of well-controlled size are also formed from cyanobacteria such as *Anabaena*, *Calothrix*, *Leptolyngbya*, etc. [113]. Moreover, several cyanobacterial strains have been used to synthesize selenium NPs (11.8 to 60 nm) [114]. Furthermore, *Spirulina subsalsa* has been utilized for the extracellular synthesis of Ag and Au NPs [115].

Very few studies on the above have suggested that these NPs could be used for the treatment of cancer (Table 2). Recently, silver NPs (AgNPs) synthesized from the aqueous extract of *Oscillatoria limnetica* have exhibited cytotoxic effects against human breast (MCF-7) and colon (HCT-116) cancer cell lines with IC<sub>50</sub> values of 6.15 µg/mL and 5.37 µg/mL, respectively [116]. In another study, silver nanoparticles (20–50 nm size) synthesized from *L. majuscula* were screened against three leukemic cell lines, i.e., K562, MOLT-3, and REH, and showed dose- and time-dependent anticancer activity. The REH cells showed the maximum sensitivity to AgNPs, with an IC<sub>50</sub> value of 620 ± 3.73 µg/mL [117]. Moreover, AgNPs (51–100 nm size) synthesized from the cell extract of the cyanobacterium *Nostoc* sp. strain HKAR-2 showed a dose-dependent cytotoxic activity against MCF-7 cancer cell lines, with an IC<sub>50</sub> of 27.5 µg/mL [118]. The phycocyanin extracted from *Nostoc linckia* synthesizes silver nanoparticles (9.39 to 25.89 nm). These AgNPs exhibit in vitro antitumor activity against the human breast MCF-7 cancer cell line (IC<sub>50</sub> = 27.79 ± 2.3 µg/mL), and were shown in vivo to inhibit tumor growth in Ehrlich ascites carcinoma-bearing mice [111]. ZnO NPs synthesized by using the cell extract of the *Nostoc* sp. EA03 exhibit less cytotoxicity when used in lower concentrations against the human adenocarcinoma alveolar basal epithelial cells (A549 cells) and human lung fibroblast (MRC-5 cells) cancer cell lines [119].

Cells and inhibited tumor growth. Consequently, they showed notable effects as anticancer agents and could be used as nanomedicines in cancer research. However, some cyanobacterial nanoformulations could also be used to deliver therapeutic drugs

to cancer sites and monitor the tumor tissues, but limited data are available. As mentioned above, numerous studies show that, even at pico to nano molar concentrations, several cyanobacterial secondary metabolites, such as apratoxin, calothrixin, curacin A, dolastatins, etc., are effective, and have shown potent inhibition of several cancer cell lines in vitro, however in vivo studies are limited. As with camptothecin, whose clinical application is limited due to its low solubility, although it has shown potent anticancer activity in vitro [120,121], most compounds isolated from cyanobacteria have a low solubility in water, which makes their formulation troublesome or even incomprehensible [122,123]. Nanoformulation of cyanobacterial compounds represents an interesting strategy to overcome the hydrophobicity or low aqueous solubility of most natural bioactive compounds. Although further studies are needed to prove the concept, it can be hypothesized that if one of these compounds is combined with a nanomaterial, as stated above, such as gold, silver, zinc, etc., it could prove more effective. Furthermore, the use of nanomedicines has unique advantages over the systemic administration of free natural bioactive molecules. These advantages include the improved protection of the biological activities of the agents in a serum-rich environment, longer periods of circulation in the blood, improved permeability and effectiveness of tumor targeting, reduction of adverse effects and the possibility of considering reactivity to stimuli for personalized therapies, etc. [122–124]. Once encapsulated in nanoparticles, the hydrophobic bioactive compound becomes completely dispersible in water and can therefore be injected intravenously; the drug-loaded nanoparticles will then be able to release the active ingredient. However, only a very few studies have used this strategy with cyanobacterial compounds, which include nanovectorized extracts from *Arthrospira platensis* with anti-fungal biofilm activity [125] and the anti-inflammatory protein phycocyanin from *Aphanizomenon flosaquae* (a freshwater cyanobacteria usually known as AFA Klamath), the delivery of which to the deep skin layers was improved when using propylene glycol-containing nanovesicles [126]. However, no attempt to nanovectorise a cyanobacterial compound with an anticancer effect has been reported to date and this would merit future research.

**Table 2.** Anticancer potential of some nanoparticles synthesized from different cyanobacterial strains.

Cyanobacterial Strain	Type of Nanoparticles	Cancer Cell Lines	IC <sub>50</sub> Value	References
<i>Oscillatoria limnetica</i>	AgNPs	MCF-7, HCT-116	6.15 and 5.37 µg/mL	[111]
<i>Lyngbya majuscula</i>	AgNPs	K562, MOLT-3, REH	620 ± 3.73 µg/mL	[119]
<i>Nostoc</i> sp. strain HKAR-2	AgNPs	MCF-7	27.5 µg/mL	[124]
<i>Nostoc linckia</i>	AgNPs	MCF-7	27.79 ± 2.3 µg/mL	[127]
<i>Nostoc</i> sp. EA03	ZnO	A549, MRC-5		[127]

Previously, green carbon nanotags (G-tags) developed from cyanobacteria were shown to be an advanced and efficient imaging platform for anticancer therapy due to their high solubility, excellent photostability and low cytotoxicity. These nanotags, when conjugated with doxorubicin, not only induced cell death in cancer cells (HepG2 and MCF-7), but also, the fluorescence of G-tags enables the monitoring of doxorubicin uptake by cancer cells and their intracellular location [127]. Similar studies could also be carried forward by conjugating cyanobacterial metabolites with nanotags, or the nanovectorization of canonical anticancer drugs using cyanobacteria to enhance the anticancer potential of the drug. Cyanobacterial metabolites from *Spirulina* showed protective effects against the cardiotoxicity induced by doxorubicin, and thus improve the therapeutic index of doxorubicin [128]. Similarly, the biochemical protective effects of *Spirulina platensis* against oxidative stress caused by doxorubicin were also evaluated [129]. These could find future applicability, with a better shelf-life and stability as natural capping occurs [130].

#### 4. Conclusions

In the last few decades, the use of cyanobacteria as a novel source of therapeutics has been realized. Several chemically diverse compounds have been screened against

different cancer cell lines, but still, very few cyanobacterial compounds have entered clinical trials, as much is not known at the molecular level. Though their economic cultivation expanded their utilization in drug discovery, still there is a need to explore more deeply into cyanobacterial compounds in order to clarify the specific targets and the mechanisms involved in cancer. Thus, more scientific attention and interdisciplinary research would have to be devoted to finding novel compounds by exploring cyanobacterial strains from extreme unexplored habitats. Furthermore, we do not explore in this review paper the structure–function relationship that might be established and would link a structural motif to a particular target. To this end, the reader may refer to the comprehensive review published previously by Salvador-Reyes and Luesch [131], which details the mechanisms of action of cyanobacterial metabolites alongside the methodology used for these discoveries. Besides this, Xu et al. focused on calothrixins synthesis and their biological effects [27]. For example, quinone compounds such as calothrixin A and B are known to be redox-active, and the generation of ROS through redox cycling of the quinone was thought to be responsible of the induced apoptosis and DNA damage [27]. Structure–function studies showed that this mechanism of action was independent of the presence of calothrixin's ring E, but strongly dependent on the tetracyclic ring quinone structure [27]. Further analyses highlighted the crucial role of the nitrogen in ring D, the importance of ring A–D, and finally evidenced the higher potential of calothrixin B [27].

One of the main subjects of interest in the field of natural biomedicines and their nanoformulations is their toxicity and/or that of contaminating toxic substances. Indeed, cyanobacteria could also be the sources of toxin production [86]. Although generally free of contaminants, cyanobacterial products may contain substances harmful to the liver, such as microcystins, toxic metals and other types of harmful bacteria, which are dangerous for human consumption [132]. Contaminated cyanobacteria can cause liver damage, stomach pain, nausea, vomiting, weakness, thirst, rapid heartbeat, shock and even death. The presence of microcystins is well known for its hepatotoxicity [132], and several other compounds cause severe anaphylaxis and neuromuscular toxicity [133]. This biosafety issue may partly explain the very low number of cyanobacterial compounds reaching clinical trials, mainly Brentuximab vedotin for Hodgkin lymphoma and Glematumumab vedotin for various cancers (Table S1) [6]. Although this is also true for numerous other compounds that exhibit strong anticancer activity but did not reach clinical trial, this might be due to their toxic nature, which hindered the biological activities in vivo or their natural contamination with toxicants while processing the drug.

In addition, the biosynthesis of NP by cyanobacteria is a relatively new idea to which promising results are attributed and, in the future, it will be possible to build datasets for marine pharmaceuticals by developing nanoformulated drugs based on cyanobacteria. However, to bring it to the platform of drug development there is a need to optimize biosynthesis pathways involving the futuristic approach of green synthesis by controlling the size and shape of particles and achieving monodispersity in the solution phase. As cyanobacteria act as natural therapeutic and have pharmaceutical potential, it could be expected that they could be used as an antitumor killer for a better world.

**Supplementary Materials:** The following are available online. Table S1: Clinical trials involving cyanobacterial-derived compounds.

**Author Contributions:** Conceptualization, H.Q., K.H. and T.H.; writing—original draft preparation, H.Q., K.H., A.S., A.K. and T.H.; writing—review and editing, T.H. and B.C.; supervision T.H. and B.C. All authors have read and agreed to the published version of the manuscript.

**Funding:** BC's research on anticancer effect of microalgae is supported by the Ligue Contre le Cancer, Comité de la Sarthe (project IRAPIM).

**Institutional Review Board Statement:** Not applicable.

**Informed Consent Statement:** Not applicable.

**Acknowledgments:** All co-authors are very thankful to their respective Dept. and School at University/Institution for all the moral support and encouragement. We are grateful to Apolline Chénais for the computer drawing enhancement of Figure 1.

**Conflicts of Interest:** The authors declare no conflict of interest. The funders had no role in the design of the study; in the collection, analyses, or interpretation of data; in the writing of the manuscript, or in the decision to publish the results.

## References

- Schopf, J.W.; Packer, B.M. Early archaen (3.3-billion to 3.5-billion-year-old) microfossils from Warrawoona group, Australia. *Science* **1987**, *237*, 70–73. [\[CrossRef\]](#) [\[PubMed\]](#)
- Singh, R.K.; Tiwari, S.P.; Rai, A.K.; Mohapatra, T.M. Cyanobacteria: An emerging source for drug discovery. *J. Antibiot.* **2011**, *64*, 401–412. [\[CrossRef\]](#) [\[PubMed\]](#)
- Gerwick, W.H.; Coates, R.C.; Engene, N.; Gerwick, L.; Grindberg, R.V.; Jones, A.C.; Sorrels, C.M. Giant marine cyanobacteria produce exciting potential pharmaceuticals. *Microbe* **2008**, *3*, 277–284. [\[CrossRef\]](#)
- Costa, M.; Costa-Rodrigues, J.; Fernandes, M.H.; Barros, P.; Vasconcelos, V.; Martins, R. Marine cyanobacteria compounds with anticancer properties: A review on the implication of apoptosis. *Mar. Drugs* **2012**, *10*, 2181–2207. [\[CrossRef\]](#) [\[PubMed\]](#)
- Liu, X.J.; Chen, F. Cell differentiation and colony alteration of *Nostoc flagelliforme*, an edible terrestrial cyanobacterium in different liquid suspension culture. *Folia Microbiol.* **2003**, *48*, 619–625. [\[CrossRef\]](#)
- Bajpai, V.K.; Shukla, S.; Kang, S.-M.; Hwang, S.K.; Song, X.; Huh, Y.S.; Han, Y.-K. Developments of cyanobacteria for nano-marine drugs: Relevance of nanoformulations in cancer therapies. *Mar. Drugs* **2018**, *16*, 179. [\[CrossRef\]](#)
- Wang, L.; Phan, D.D.; Zhang, J.; Ong, P.S.; Thuya, W.L.; Soo, R.; Wong, A.L.; Yong, W.P.; Lee, S.C.; Ho, P.C.; et al. Anticancer properties of nimbolide and pharmacokinetic considerations to accelerate its development. *Oncotarget* **2016**, *7*, 44790–44802. [\[CrossRef\]](#)
- Andrianasolo, E.H.; Gross, H.; Goeger, D.; Musafija-Girt, M.; McPhail, K.; Leal, R.M.; Mooberry, S.L.; Gerwick, W.H. Isolation of swinholid A and related glycosylated derivatives from two field collections of marine cyanobacteria. *Org. Lett.* **2005**, *7*, 1375–1378. [\[CrossRef\]](#)
- Luesch, H.; Chanda, S.K.; Raya, R.M.; DeJesus, P.D.; Orth, A.P.; Walker, J.R.; Belmonte, J.C.I.; Schultz, P.G. A functional genomics approach to the mode of action of apratoxin A. *Nat. Chem. Biol.* **2006**, *2*, 158–167. [\[CrossRef\]](#)
- Liu, Y.; Law, B.K.; Luesch, H. Apratoxin A reversibly inhibits the secretory pathway by preventing cotranslational translocation. *Mol. Pharmacol.* **2009**, *76*, 91–104. [\[CrossRef\]](#)
- Luesch, H.; Yoshida, W.Y.; Moore, R.E.; Paul, V.J.; Corbett, T.H. Total structure determination of apratoxin A, a potent cytotoxin from the marine cyanobacterium *Lyngbya majuscula*. *J. Am. Chem. Soc.* **2001**, *123*, 5418–5423. [\[CrossRef\]](#) [\[PubMed\]](#)
- Chen, Q.Y.; Liu, Y.; Luesch, H. Systematic chemical mutagenesis identifies a potent novel apratoxin A/E hybrid with improved in vivo antitumor activity. *ACS Med. Chem. Lett.* **2011**, *2*, 861–865. [\[CrossRef\]](#) [\[PubMed\]](#)
- Shen, S.; Zhang, P.; Lovchik, M.A.; Li, Y.; Tang, L.; Chen, Z.; Zeng, R.; Ma, D.; Yuan, J.; Yu, Q. Cyclodepsipeptide toxin promotes the degradation of Hsp90 client proteins through chaperone-mediated autophagy. *J. Cell Biol.* **2009**, *185*, 629–639. [\[CrossRef\]](#) [\[PubMed\]](#)
- Huang, K.-C.; Chen, Z.; Jiang, Y.; Akare, S.; Kolber-Simonds, D.; Condon, K.; Agoulnik, S.; Tendyke, K.; Shen, Y.; Wu, K.-M.; et al. Apratoxin A shows novel pancreas-targeting activity through the binding of sec 61. *Mol. Cancer Ther.* **2016**, *15*, 1208–1216. [\[CrossRef\]](#) [\[PubMed\]](#)
- Cai, W.; Ratnayake, R.; Gerber, M.H.; Chen, Q.Y.; Yu, Y.; Derendorf, H.; Trevino, J.G.; Luesch, H. Development of apratoxin S10 (Apra S10) as an anti-pancreatic cancer agent and its preliminary evaluation in an orthotopic patient-derived xenograft (PDX) model. *Invest. New Drugs* **2019**, *37*, 364–374. [\[CrossRef\]](#)
- Gutierrez, M.; Suyama, T.L.; Engene, N.; Wingerd, J.S.; Matainaho, T.; Gerwick, W.H. Apratoxin D, a potent cytotoxic cyclodepsipeptide from Papua-New-Guinea collections of the marine cyanobacteria *Lyngbya majuscula* and *Lyngbya sordida*. *J. Nat. Prod.* **2008**, *71*, 1099–1103. [\[CrossRef\]](#)
- Han, B.; Gross, H.; Goeger, D.E.; Mooberry, S.L.; Gerwick, W.H. Aurilides B and C, cancer cell toxins from a Papua-New-Guinea collection of the marine cyanobacterium *Lyngbya majuscula*. *J. Nat. Prod.* **2006**, *69*, 572–575. [\[CrossRef\]](#)
- Sato, S.; Murata, A.; Orihara, T.; Shirakawa, T.; Suenaga, K.; Kigoshi, H.; Uesugi, M. Marine natural product aurilide activates the OPA1-mediated apoptosis by binding to prohibitin. *Chem. Biol.* **2011**, *18*, 131–139. [\[CrossRef\]](#)
- Sumiya, E.; Shimogawa, H.; Sasaki, H.; Tsutsumi, M.; Yoshita, K.; Ojika, M.; Suenaga, K.; Uesugi, M. Cell-morphology profiling of a natural product library identifies bisbromoamide and miuraenamides A as actin filament stabilizers. *ACS Chem. Biol.* **2011**, *6*, 425–431. [\[CrossRef\]](#)
- Teruya, T.; Sasaki, H.; Fukazawa, H.; Suenaga, K. Bisbromoamide, a potent cytotoxic peptide from the marine cyanobacterium *Lyngbya* sp.: Isolation, stereostructure, and biological activity. *Org. Lett.* **2009**, *11*, 5062–5065. [\[CrossRef\]](#)
- Li, W.; Yu, S.; Jin, M.; Xia, H.; Ma, D. Total synthesis and cytotoxicity of bisbromoamide and its analogs. *Tetrahedron Lett.* **2011**, *52*, 2124–2127. [\[CrossRef\]](#)
- Suzuki, K.; Mizuno, R.; Suenaga, K.; Kosaka, T.; Tanaka, N.; Shinoda, K.; Kono, H.; Kikuchi, E.; Nagata, H.; Asanuma, H.; et al. 307 Bisbromoamide, as a novel molecular target drug inhibiting phosphorylation of both extracellular signal-regulated kinase and AKT in renal cell carcinoma. *J. Urol.* **2012**, *187*, 124–125. [\[CrossRef\]](#)



23. Suzuki, K.; Mizuno, R.; Suenaga, K.; Teruya, T.; Tanaka, N.; Kosaka, T.; Oya, M. Bisebromoamide, an extract from *Lyngbya* species, induces apoptosis through ERK and mTOR inhibitions in renal cancer cells. *Cancer Med.* **2013**, *2*, 32–39. [\[CrossRef\]](#)
24. Teruya, T.; Sasaki, H.; Kitamura, K.; Nakayama, T.; Suenaga, K. Biselyngbyaside, a macrolide glycoside from the marine cyanobacterium *Lyngbya* sp. *Org. Lett.* **2009**, *11*, 2421–2424. [\[CrossRef\]](#) [\[PubMed\]](#)
25. Watanabe, A.; Ohno, O.; Morita, M.; Inuzuka, T.; Suenaga, K. Structures and biological activities of novel biselyngbyaside analogs isolated from the marine cyanobacterium *Lyngbya* sp. *Bull. Chem. Soc. Jpn.* **2015**, *88*, 1256–1264. [\[CrossRef\]](#)
26. Banker, R.; Carmeli, S. Tenucyclamides A-D, cyclic hexapeptides from the cyanobacterium *Nostoc spongiaeforme* var. *tenue*. *J. Nat. Prod.* **1998**, *61*, 1248–1251. [\[CrossRef\]](#)
27. Xu, S.; Nijampatnam, B.; Dutta, S.; Velu, S.E. Cyanobacterial metabolite calothrixins: Recent advances in synthesis and biological evaluation. *Mar. Drugs* **2016**, *14*, 17. [\[CrossRef\]](#)
28. Chen, X.X.; Smith, G.D.; Waring, P. Human cancer cell (Jurkat) killing by the cyanobacterial metabolite calothrixin A. *J. Appl. Phycol.* **2003**, *15*, 269–277. [\[CrossRef\]](#)
29. Hatae, N.; Satoh, R.; Chiba, H.; Osaki, T.; Nishiyama, T.; Ishikura, M.; Abe, T.; Hibino, S.; Choshi, T.; Okada, C. N-Substituted calothrixin B derivatives inhibited the proliferation of HL-60 promyelocytic leukemia cells. *Med. Chem. Res.* **2014**, *23*, 4956–4961. [\[CrossRef\]](#)
30. Ramalingam, B.M.; Moorthy, N.D.; Chowdhury, S.R.; Mageshwaran, T.; Vellaichamy, E.; Saha, S.; Ganesan, K.; Rajesh, B.N.; Iqbal, S.; Majumder, H.K.; et al. Synthesis and biological evaluation of calothrixins B and their deoxygenated analogs. *J. Med. Chem.* **2018**, *61*, 1285–1315. [\[CrossRef\]](#)
31. Moorthy, N.D.; Ramalingam, B.M.; Iqbal, S.; Mohanakrishnan, A.K.; Gunasekaran, K.; Vellaichamy, E. Novel isothiacalothrixin B analogs exhibit cytotoxic activity on human colon cancer cells in vitro by inducing irreversible DNA damage. *PLoS ONE* **2018**, *13*, e0202903. [\[CrossRef\]](#)
32. Pereira, A.R.; Kale, A.J.; Fenley, A.T.; Byrum, T.; Debonsi, H.M.; Gilson, M.K.; Valeriote, F.A.; Moore, B.S.; Gerwick, W.H. The carmaphyccins: New proteasome inhibitors exhibiting an  $\alpha,\beta$ -epoxyketone warhead from a marine cyanobacterium. *ChemBioChem* **2012**, *13*, 810–817. [\[CrossRef\]](#)
33. Almaliti, J.; Miller, B.; Pietraszkiewicz, H.; Glukhov, E.; Naman, C.B.; Kline, T.; Hanson, J.; Li, X.; Zhou, S.; Valeriote, F.A.; et al. Exploration of the carmaphyccins as payloads in antibody drug conjugate anticancer agents. *Eur. J. Med. Chem.* **2019**, *161*, 416–432. [\[CrossRef\]](#)
34. MacMillan, J.B.; Molinski, T.F. Caylobolide A, a unique 36-membered macrolactone from a Bahamian *Lyngbya majuscula*. *Org. Lett.* **2002**, *4*, 1535–1538. [\[CrossRef\]](#) [\[PubMed\]](#)
35. Salvador, L.A.; Paul, V.J.; Luesch, H. Caylobolide B, a macrolactone from symplostatin 1-producing marine cyanobacteria *Phormidium* spp. from Florida. *J. Nat. Prod.* **2010**, *73*, 1606–1609. [\[CrossRef\]](#) [\[PubMed\]](#)
36. Hau, A.M.; Greenwood, J.A.; Löhr, C.V.; Serrill, J.D.; Proteau, P.J.; Ganley, I.G.; McPhail, K.L.; Ishmael, J.E. Coibamide A induces mTOR-independent autophagy and cell death in human glioblastoma cells. *PLoS ONE* **2013**, *8*, e65250. [\[CrossRef\]](#) [\[PubMed\]](#)
37. Medina, R.A.; Goeger, D.E.; Hills, P.; Mooberry, S.L.; Huang, N.; Romero, L.I.; Ortega-Barría, E.; Gerwick, W.H.; McPhail, K.L. Coibamide, A potent antiproliferative cyclic depsipeptide from the Panamanian marine cyanobacterium *Leptolyngbya* sp. *J. Am. Chem. Soc.* **2008**, *130*, 6324–6325. [\[CrossRef\]](#) [\[PubMed\]](#)
38. Yao, G.; Wang, W.; Ao, L.; Cheng, Z.; Wu, C.; Pan, Z.; Liu, K.; Li, H.; Su, W.; Fang, L. Improved total synthesis and biological evaluation of coibamide A analogues. *J. Med. Chem.* **2018**, *61*, 8908–8916. [\[CrossRef\]](#)
39. Moore, R.E. Cyclic peptides and depsipeptides from cyanobacteria: A review. *J. Ind. Microbiol.* **1996**, *16*, 134–143. [\[CrossRef\]](#)
40. Kang, H.K.; Choi, M.C.; Seo, C.H.; Park, Y. Therapeutic properties and biological benefits of marine-derived anticancer peptides. *Int. J. Mol. Sci.* **2018**, *19*, 919. [\[CrossRef\]](#)
41. Drew, L.; Fine, R.L.; Do, T.N.; Douglas, G.P.; Petrylak, D.P. The novel antimicrotubule agent cryptophycin 52 (LY355703) induces apoptosis via multiple pathways in human prostate cancer cells. *Clin. Cancer Res.* **2002**, *8*, 3922–3932. [\[PubMed\]](#)
42. D’Agostino, G.; del Campo, J.; Mellado, B.; Izquierdo, M.A.; Minarik, T.; Cirri, L.; Marini, L.; Perez-Gracia, J.L.; Scambia, G. A multicenter phase II study of the cryptophycin analog LY355703 in patients with platinum-resistant ovarian cancer. *Int. J. Gynecol. Cancer.* **2006**, *16*, 71–76. [\[CrossRef\]](#) [\[PubMed\]](#)
43. Weiss, C.; Figueras, E.; Borbély, A.N.; Sewald, N. Cryptophycins: Cytotoxic cyclodepsipeptides with potential for tumor targeting. *J. Pept. Sci.* **2017**, *23*, 514–531. [\[CrossRef\]](#) [\[PubMed\]](#)
44. Borbély, A.; Figueras, E.; Martins, A.; Boderio, L.; Dias, A.R.M.; Rivas, P.L.; Pina, A.; Arosio, D.; Gallinari, P.; Frese, M.; et al. Conjugates of cryptophycin and RGD or isoDGR peptidomimetics for targeted drug delivery. *ChemistryOpen* **2019**, *8*, 737–742. [\[CrossRef\]](#) [\[PubMed\]](#)
45. Borbély, A.; Figueras, E.; Martins, A.; Esposito, S.; Auciello, G.; Monteagudo, E.; di Marco, A.; Summa, V.; Cordella, P.; Perego, R.; et al. Synthesis and biological evaluation of RGD-cryptophycin conjugates for targeted drug delivery. *Pharmaceutics* **2019**, *11*, 151. [\[CrossRef\]](#) [\[PubMed\]](#)
46. Simmons, T.L.; Andrianasolo, E.; McPhail, K.; Flatt, P.; Gerwick, W.H. Marine natural products as anticancer drugs. *Mol. Cancer Ther.* **2005**, *4*, 333–342. [\[PubMed\]](#)
47. El-Hack, M.E.A.; Abdelnour, S.; Alagawany, M.; Abdo, M.; Sakr, M.A.; Khafaga, A.F.; Mahgoub, S.A.; Elnesr, S.S.; Gebriel, M.G. Microalgae in modern cancer therapy: Current knowledge. *Biomed. Pharmacother.* **2019**, *111*, 42–50. [\[CrossRef\]](#) [\[PubMed\]](#)

48. Simmons, T.L.; Nogle, L.M.; Media, J.; Valeriote, F.A.; Mooberry, S.L.; Gerwick, W.H. Desmethoxymajusculamide C, a cyanobacterial depsipeptide with potent cytotoxicity in both cyclic and ring-opened forms. *J. Nat. Prod.* **2009**, *72*, 1011–1016. [\[CrossRef\]](#)
49. Luesch, H.; Moore, R.E.; Paul, V.J.; Mooberry, S.L.; Corbett, T.H. Isolation of dolastatin 10 from the marine cyanobacterium *Symploca* species VP642 and total stereochemistry and biological evaluation of its analog symplostatatin 1. *J. Nat. Prod.* **2001**, *64*, 907–910. [\[CrossRef\]](#)
50. Luesch, H.; Yoshida, W.Y.; Moore, R.E.; Paul, V.J.; Mooberry, S.L.; Corbett, T.H. Symplostatatin 3, a new dolastatin 10 analogue from the marine cyanobacterium *Symploca* sp. VP452. *J. Nat. Prod.* **2002**, *65*, 16–20. [\[CrossRef\]](#)
51. Deng, C.; Pan, B.; O'Connor, O.A. Brentuximab vedotin. *Clin. Cancer Res.* **2013**, *19*, 22–27. [\[CrossRef\]](#) [\[PubMed\]](#)
52. Gerwick, W.H.; Moore, B.S. Lessons from the past and charting the future of marine natural products drug discovery and chemical biology. *Chem. Biol.* **2012**, *19*, 85–98. [\[CrossRef\]](#) [\[PubMed\]](#)
53. Ott, P.A.; Pavlick, A.C.; Johnson, D.B.; Hart, L.L.; Infante, J.R.; Luke, J.J.; Lutzky, J.; Rothschild, N.; Spitler, L.; Cowey, C.L. A phase 2 study of glembatumumab vedotin (GV), an antibody-drug conjugate (ADC) targeting gpNMB, in advanced melanoma. *Ann. Oncol.* **2016**, *27*, e1147. [\[CrossRef\]](#)
54. Pettit, G.R.; Hogan, F.; Toms, S. Antineoplastic agents. 592. Highly effective cancer cell growth inhibitory structural modifications of dolastatin 10. *J. Nat. Prod.* **2011**, *74*, 962–968. [\[CrossRef\]](#)
55. Gianolio, D.A.; Rouleau, C.; Bauta, W.E.; Lovett, D.; Cantrell, W.R., Jr.; Recio, A., III; Wolstenholme-Hogg, P.; Busch, M.; Pan, P.; Stefano, J.E.; et al. Targeting HER2-positive cancer with dolastatin 15 derivatives conjugated to trastuzumab, novel antibody-drug conjugates. *Cancer Chemother. Pharmacol.* **2012**, *70*, 439–449. [\[CrossRef\]](#)
56. Yang, K.; Chen, B.; Gianolio, D.A.; Stefano, J.E.; Busch, M.; Manning, C.; Alving, K.; Gregory, R.C.; Brondyk, W.H.; Miller, R.J.; et al. Convergent synthesis of hydrophilic monomethyl dolastatin 10 based drug linkers for antibody-drug conjugation. *Org. Biomol. Chem.* **2019**, *17*, 8115–8124. [\[CrossRef\]](#)
57. Kwan, J.C.; Ratnayake, R.; Abboud, K.A.; Paul, V.J.; Luesch, H. Grassypeptolides A–C, cytotoxic bis-thiazoline containing marine cyclodepsipeptides. *J. Org. Chem.* **2010**, *75*, 8012–8023. [\[CrossRef\]](#)
58. Thornburg, C.C.; Thimmaiah, M.; Shaala, L.A.; Hau, A.M.; Malmo, J.M.; Ishmael, J.E.; Youssef, D.T.; McPhail, K.L. Cyclic depsipeptides, grassypeptolides D and E and Ibu-epidemethoxylyngbyastatin 3, from a Red Sea *Leptolyngbya* cyanobacterium. *J. Nat. Prod.* **2011**, *74*, 1677–1685. [\[CrossRef\]](#)
59. Tripathi, A.; Puddick, J.; Prinsep, M.R.; Lee, P.P.; Tan, L.T. Hantupeptin A, a cytotoxic cyclic depsipeptide from a Singapore collection of *Lyngbya majuscula*. *J. Nat. Prod.* **2009**, *72*, 29–32. [\[CrossRef\]](#)
60. Marquez, B.L.; Watts, K.S.; Yokochi, A.; Roberts, M.A.; Verdier-Pinard, P.; Jimenez, J.I.; Hamel, E.; Scheuer, P.J.; Gerwick, W.H. Structure and absolute stereochemistry of hectochlorin, a potent stimulator of actin assembly. *J. Nat. Prod.* **2002**, *65*, 866–871. [\[CrossRef\]](#)
61. Leao, P.N.; Costa, M.; Ramos, V.; Pereira, A.R.; Fernandes, V.C.; Domingues, V.F.; Gerwick, W.H.; Vasconcelos, V.M.; Martins, R. Antitumor activity of hierridin B, a cyanobacterial secondary metabolite found in both filamentous and unicellular marine strains. *PLoS ONE* **2013**, *8*, e69562. [\[CrossRef\]](#) [\[PubMed\]](#)
62. Malloy, K.L.; Choi, H.; Fiorilla, C.; Valeriote, F.A.; Matainaho, T.; Gerwick, W.H. Hoiamide D, a marine cyanobacteria-derived inhibitor of p53/MDM2 interaction. *Bioorg. Med. Chem. Lett.* **2012**, *22*, 683–688. [\[CrossRef\]](#) [\[PubMed\]](#)
63. Jimenez, J.I.; Vansach, T.; Yoshida, W.Y.; Sakamoto, B.; Porzgen, P.; Horgen, F.D. Halogenated fatty acid amides and cyclic depsipeptides from an eastern Caribbean collection of the cyanobacterium *Lyngbya majuscula*. *J. Nat. Prod.* **2009**, *72*, 1573–1578. [\[CrossRef\]](#) [\[PubMed\]](#)
64. Tripathi, A.; Fang, W.; Leong, D.T.; Tan, L.T. Biochemical studies of the lagunamides, potent cytotoxic cyclic depsipeptides from the marine cyanobacterium *Lyngbya majuscula*. *Mar. Drugs* **2012**, *10*, 1126–1137. [\[CrossRef\]](#) [\[PubMed\]](#)
65. Tripathi, A.; Puddick, J.; Prinsep, M.R.; Rottmann, M.; Tan, L.T. Lagunamides A and B: Cytotoxic and antimalarial cyclodepsipeptides from the marine cyanobacterium *Lyngbya majuscula*. *J. Nat. Prod.* **2010**, *73*, 1810–1814. [\[CrossRef\]](#)
66. Tripathi, A.; Puddick, J.; Prinsep, M.R.; Rottmann, M.; Chan, K.P.; Chen, D.Y.; Tan, L.T. Lagunamide C, a cytotoxic cyclodepsipeptide from the marine cyanobacterium *Lyngbya majuscula*. *Phytochemistry* **2011**, *72*, 2369–2375. [\[CrossRef\]](#) [\[PubMed\]](#)
67. Luo, D.; Putra, M.Y.; Ye, T.; Paul, V.J.; Luesch, H. Isolation, structure elucidation and biological evaluation of lagunamide D: A new cytotoxic macrocyclic depsipeptide from marine cyanobacteria. *Mar. Drugs* **2019**, *17*, 83. [\[CrossRef\]](#) [\[PubMed\]](#)
68. Huang, X.; Huang, W.; Li, L.; Sun, X.; Song, S.; Xu, Q.; Zhang, L.; Wei, B.G.; Deng, X. Structure determinants of lagunamide A for anticancer activity and its molecular mechanism of mitochondrial apoptosis. *Mol. Pharm.* **2016**, *13*, 3756–3763. [\[CrossRef\]](#)
69. Taori, K.; Paul, V.J.; Luesch, H. Structure and activity of largazole, a potent antiproliferative agent from the Floridian marine cyanobacterium *Symploca* sp. *J. Am. Chem. Soc.* **2008**, *130*, 1806–1807. [\[CrossRef\]](#)
70. Liu, Y.; Salvador, L.A.; Byeon, S.; Ying, Y.; Kwan, J.C.; Law, B.K.; Hong, J.; Luesch, H. Anticancer activity of largazole, a marine-derived tunable histone deacetylase inhibitor. *J. Pharmacol. Exp. Ther.* **2010**, *335*, 351–361. [\[CrossRef\]](#)
71. Lee, S.U.; Kwak, H.B.; Pi, S.H.; You, H.K.; Byeon, S.R.; Ying, Y.; Luesch, H.; Hong, J.; Kim, S.H. In vitro and in vivo osteogenic activity of largazole. *ACS Med. Chem. Lett.* **2011**, *2*, 248–251. [\[CrossRef\]](#)
72. Liu, Y.; Wang, Z.; Wang, J.; Lam, W.; Kwong, S.; Li, F.; Friedman, S.L.; Zhou, S.; Ren, Q.; Xu, Z.; et al. A histone deacetylase inhibitor, largazole, decreases liver fibrosis and angiogenesis by inhibiting transforming growth factor- $\beta$  and vascular endothelial growth factor signaling. *Liver Int.* **2013**, *33*, 504–515. [\[CrossRef\]](#) [\[PubMed\]](#)



73. Law, M.E.; Corsino, P.E.; Jahn, S.C.; Davis, B.J.; Chen, S.; Patel, B.; Pham, K.; Lu, J.; Sheppard, B.; Nørgaard, P.; et al. Glucocorticoids and histone deacetylase inhibitors cooperate to block the invasiveness of basal-like breast cancer cells through novel mechanisms. *Oncogene* **2013**, *32*, 1316–1329. [[CrossRef](#)] [[PubMed](#)]
74. Ghosh, S.K.; Perrine, S.P.; Williams, R.M.; Faller, D.V. Histone deacetylase inhibitors are potent inducers of gene expression in latent EBV and sensitize lymphoma cells to nucleoside antiviral agents. *Blood* **2012**, *119*, 1008–1017. [[CrossRef](#)] [[PubMed](#)]
75. Ungermannova, D.; Parker, S.J.; Nasveschuk, C.G.; Wang, W.; Quade, B.; Zhang, G.; Kuchta, R.D.; Phillips, A.J.; Liu, X. Largazole and its derivatives selectively inhibit ubiquitin activating enzyme (E1). *PLoS ONE* **2012**, *7*, e29208. [[CrossRef](#)] [[PubMed](#)]
76. Bonnard, I.; Rolland, M.; Salmon, J.-M.; Debiton, E.; Barthomeuf, C.; Banaigs, B. Total structure and inhibition of tumor cell proliferation of laxaphycins. *J. Med. Chem.* **2007**, *50*, 1266–1279. [[CrossRef](#)] [[PubMed](#)]
77. Cai, W.; Matthew, S.; Chen, Q.-Y.; Paul, V.J.; Luesch, H. Discovery of new A- and B-type laxaphycins with synergistic anticancer activity. *Bioorg. Med. Chem.* **2018**, *26*, 2310–2319. [[CrossRef](#)] [[PubMed](#)]
78. Luesch, H.; Yoshida, W.Y.; Moore, R.E.; Paul, V.J.; Mooberry, S.L. Isolation, structure determination, and biological activity of lyngbyabellin A from the marine cyanobacterium *Lyngbya majuscula*. *J. Nat. Prod.* **2000**, *63*, 611–615. [[CrossRef](#)]
79. Luesch, H.; Yoshida, W.Y.; Moore, R.E.; Paul, V.J. Isolation and structure of the cytotoxin lyngbyabellin B and absolute configuration of lyngbyapeptin A from the marine cyanobacterium *Lyngbya majuscula*. *J. Nat. Prod.* **2000**, *63*, 1437–1439. [[CrossRef](#)]
80. Han, B.; McPhail, K.L.; Gross, H.; Goeger, D.E.; Mooberry, S.L.; Gerwick, W.H. Isolation and structure of five lyngbyabellin derivatives from a Papua New Guinea collection of the marine cyanobacterium *Lyngbya majuscula*. *Tetrahedron* **2005**, *61*, 11723–11729. [[CrossRef](#)]
81. Choi, H.; Mevers, E.; Byrum, T.; Valeriote, F.A.; Gerwick, W.H. Lyngbyabellins K-N from two palmyra atoll collections of the marine cyanobacterium *Moorea bouillonii*. *Eur. J. Org. Chem.* **2012**, *2012*, 5141–5150. [[CrossRef](#)]
82. Matthew, S.; Ross, C.; Rocca, J.R.; Paul, V.J.; Luesch, H. Lyngbyastatin 4, a dolastatin 13 analog with elastase and chymotrypsin inhibitory activity from the marine cyanobacterium *Lyngbya confervoides*. *J. Nat. Prod.* **2007**, *70*, 124–127. [[CrossRef](#)] [[PubMed](#)]
83. Kwan, J.C.; Taori, K.; Paul, V.J.; Luesch, H. Lyngbyastatins 8–10, elastase inhibitors with cyclic depsipeptide scaffolds isolated from the marine cyanobacterium *Lyngbya semiplena*. *Mar. Drugs* **2009**, *7*, 528–538. [[CrossRef](#)] [[PubMed](#)]
84. Chang, T.T.; More, S.V.; Lu, I.H.; Hsu, J.C.; Chen, T.J.; Jen, Y.C.; Lu, C.K.; Li, W.S. Isomalyngamide A, A-1 and their analogs suppress cancer cell migration in vitro. *Eur. J. Med. Chem.* **2011**, *46*, 3810–3819. [[CrossRef](#)] [[PubMed](#)]
85. Kwan, J.C.; Teplitski, M.; Gunasekera, S.P.; Paul, V.J.; Luesch, H. Isolation and biological evaluation of 8-epi-malyngamide C from the Floridian marine cyanobacterium *Lyngbya majuscula*. *J. Nat. Prod.* **2010**, *73*, 463–466. [[CrossRef](#)]
86. Kang, H.S.; Santarsiero, B.D.; Kim, H.; Krunic, A.; Shen, Q.; Swanson, S.M.; Chai, H.; Kinghorn, A.D.; Orjala, J. Merocyclophanes A and B, antiproliferative cyclophanes from the cultured terrestrial cyanobacterium *Nostoc* sp. *Phytochemistry* **2012**, *79*, 109–115. [[CrossRef](#)]
87. Sueyoshi, K.; Yamano, A.; Ozaki, K.; Sumimoto, S.; Iwasaki, A.; Suenaga, K.; Teruya, T. Three new malyngamides from the marine cyanobacterium *Moorea producens*. *Mar. Drugs* **2017**, *15*, 367. [[CrossRef](#)]
88. Voráčová, K.; Hájek, J.; Mareš, J.; Urajová, P.; Kuzma, M.; Cheel, J.; Villunger, A.; Kapuscik, A.; Bally, M.; Novák, P.; et al. The cyanobacterial metabolite nocuolin A is a natural oxadiazine that triggers apoptosis in human cancer cells. *PLoS ONE* **2017**, *12*, e0172850. [[CrossRef](#)]
89. Montaser, R.; Paul, V.J.; Luesch, H. Pitipeptolides C-F, antimycobacterial cyclodepsipeptides from the marine cyanobacterium *Lyngbya majuscula* from Guam. *Phytochemistry* **2011**, *72*, 2068–2074. [[CrossRef](#)]
90. Stevenson, C.S.; Capper, E.A.; Roshak, A.K.; Marquez, B.; Eichman, C.; Jackson, J.R.; Mattern, M.; Gerwick, W.H.; Jacobs, R.S.; Marshall, L.A. The identification and characterization of the marine natural product scytonemin as a novel antiproliferative pharmacophore. *J. Pharmacol. Exp. Ther.* **2002**, *303*, 858–866. [[CrossRef](#)]
91. Linington, R.G.; Edwards, D.J.; Shuman, C.F.; McPhail, K.L.; Matainaho, T.; Gerwick, W.H. Symplocamide A, a potent cytotoxin and chymotrypsin inhibitor from the marine cyanobacterium *Symploca* sp. *J. Nat. Prod.* **2008**, *71*, 22–27. [[CrossRef](#)] [[PubMed](#)]
92. Williams, P.G.; Yoshida, W.Y.; Moore, R.E.; Paul, V.J. The isolation and structure elucidation of tasiamide B, a 4-amino-3-hydroxy-5-phenylpentanoic acid containing peptide from the marine cyanobacterium *Symploca* sp. *J. Nat. Prod.* **2003**, *66*, 1006–1009. [[CrossRef](#)] [[PubMed](#)]
93. Zhang, W.; Sun, T.; Ma, Z.; Li, Y. Design, synthesis and biological evaluation of tasiamide analogs as tumor inhibitors. *Mar. Drugs* **2014**, *12*, 2308–2325. [[CrossRef](#)] [[PubMed](#)]
94. Mevers, E.; Liu, W.T.; Engene, N.; Mohimani, H.; Byrum, T.; Pevzner, P.A.; Dorrestein, P.C.; Spadafora, C.; Gerwick, W.H. Cytotoxic veraguamides, alkynyl bromide-containing cyclic depsipeptides from the marine cyanobacterium cf. *Oscillatoria margaritifera*. *J. Nat. Prod.* **2011**, *74*, 928–936. [[CrossRef](#)] [[PubMed](#)]
95. Salvador, L.A.; Biggs, J.S.; Paul, V.J.; Luesch, H. Veraguamides A-G, cyclic hexadepsipeptides from a dolastatin 16-producing cyanobacterium *Symploca* cf. *hydroides* from Guam. *J. Nat. Prod.* **2011**, *74*, 917–927. [[CrossRef](#)]
96. Al-Awadhi, F.H.; Salvador, L.A.; Law, B.K.; Paul, V.J.; Luesch, H. Kempopeptin C, a novel marine-derived serine protease inhibitor targeting invasive breast cancer. *Mar. Drugs* **2017**, *15*, 290. [[CrossRef](#)]
97. Simmons, T.L.; McPhail, K.L.; Ortega-Barria, E.; Mooberry, S.L.; Gerwick, W.H. Belamide A, a new antimitotic tetrapeptide from a Panamanian marine cyanobacterium. *Tetrahedron Lett.* **2006**, *47*, 3387–3390. [[CrossRef](#)]
98. Jimenez, J.I.; Scheuer, P.J. New lipopeptides from the Caribbean cyanobacterium *Lyngbya majuscula*. *J. Nat. Prod.* **2001**, *64*, 200–203. [[CrossRef](#)]

99. Ahmed, B.E.; Badawi, M.H.; Mostafa, S.S.; Higazy, A.M. Human anticancer and antidiabetic activities of the cyanobacterium *Fischerella* sp. BS1-EG isolated from River Nile, Egypt. *Int. J. Curr. Microbiol. Appl. Sci.* **2018**, *7*, 3473–3485. [\[CrossRef\]](#)
100. Horgen, F.D.; Kazmierski, E.B.; Westenburg, H.E.; Yoshida, W.Y.; Scheuer, P.J. Malevamide D: Isolation and structure determination of an isodolastatin H analog from the marine cyanobacterium *Symploca hydroides*. *J. Nat. Prod.* **2002**, *65*, 487–491. [\[CrossRef\]](#)
101. Wrasidlo, W.; Mielgo, A.; Torres, V.A.; Barbero, S.; Stoletov, K.; Suyama, T.L.; Klemke, R.L.; Gerwick, W.H.; Carson, D.A.; Stupack, D.G. The marine lipopeptide somocystinamide A triggers apoptosis via caspase 8. *Proc. Natl. Acad. Sci. USA* **2008**, *105*, 2313–2318. [\[CrossRef\]](#) [\[PubMed\]](#)
102. Matthew, S.; Paul, V.J.; Luesch, H. Tiglicamides A–C, cyclodepsipeptides from the marine cyanobacterium *Lyngbya confervoides*. *Phytochemistry* **2009**, *70*, 2058–2063. [\[CrossRef\]](#) [\[PubMed\]](#)
103. Williams, P.G.; Yoshida, W.Y.; Quon, M.K.; Moore, R.E.; Paul, V.J. Ulongapeptin, a cytotoxic cyclic depsipeptide from a Palauan marine cyanobacterium *Lyngbya* sp. *J. Nat. Prod.* **2003**, *66*, 651–654. [\[CrossRef\]](#) [\[PubMed\]](#)
104. Williams, P.G.; Yoshida, W.Y.; Moore, R.E.; Paul, V.J. Isolation and structure determination of obyanamide, a novel cytotoxic cyclic depsipeptide from the marine cyanobacterium *Lyngbya confervoides*. *J. Nat. Prod.* **2002**, *65*, 29–31. [\[CrossRef\]](#)
105. Han, B.; Goeger, D.; Maier, C.S.; Gerwick, W.H. The wewakpeptins, cyclic depsipeptides from a Papua New Guinea collection of the marine cyanobacterium *Lyngbya semiplena*. *J. Org. Chem.* **2005**, *70*, 3133–3139. [\[CrossRef\]](#)
106. Davies-Coleman, M.T.; Dzeha, T.M.; Gray, C.A.; Hess, S.; Pannell, L.K.; Hendricks, D.T.; Arendse, C.E. Isolation of homodolastatin 16, a new cyclic depsipeptide from a Kenyan collection of *Lyngbya majuscula*. *J. Nat. Prod.* **2003**, *66*, 712–715. [\[CrossRef\]](#) [\[PubMed\]](#)
107. Edwards, D.J.; Marquez, B.L.; Nogle, L.M.; McPhail, K.; Goeger, D.E.; Roberts, M.A.; Gerwick, W.H. Structure and biosynthesis of the jamaicamides, new mixed polyketide-peptide neurotoxins from the marine cyanobacterium *Lyngbya majuscula*. *Chem. Biol.* **2004**, *11*, 817–833. [\[CrossRef\]](#)
108. Gutierrez, M.; Tidgewell, K.; Capson, T.L.; Engene, N.; Almanza, A.; Schemies, J.; Jung, M.; Gerwick, W.H. Malynolid dimer, a bioactive symmetric cyclodepside from the Panamanian marine cyanobacterium *Lyngbya majuscula*. *J. Nat. Prod.* **2010**, *73*, 709–711. [\[CrossRef\]](#)
109. Brumley, D.A.; Gunasekera, S.P.; Chen, Q.Y.; Paul, V.J.; Luesch, H. Discovery, total synthesis, and SAR of anaenamides A and B: Anticancer cyanobacterial depsipeptides with a chlorinated pharmacophore. *Org. Lett.* **2020**, *22*, 4235–4239. [\[CrossRef\]](#)
110. Keller, L.; Canuto, K.M.; Liu, C.; Suzuki, B.M.; Almaliti, J.; Sikandar, A.; Naman, C.B.; Glukhov, E.; Luo, D.; Duggan, B.M.; et al. Tutuilamides A–C: Vinyl-chloride containing cyclodepsipeptides from marine cyanobacteria with potent elastase inhibitory properties. *ACS Chem. Biol.* **2020**, *15*, 751–757. [\[CrossRef\]](#)
111. El-Naggar, N.E.; Hussein, M.H.; El-Sawah, A.A. Biofabrication of silver nanoparticles by phycocyanin, characterization, in vitro anticancer activity against breast cancer cell line and in vivo cytotoxicity. *Sci. Rep.* **2017**, *7*, 10844. [\[CrossRef\]](#) [\[PubMed\]](#)
112. Roychoudhury, P.; Ghosh, S.; Pal, R. Cyanobacteria mediated green synthesis of gold-silver nanoalloy. *J. Plant. Biochem. Biotechnol.* **2016**, *25*, 73–78. [\[CrossRef\]](#)
113. Brayner, R.; Barberousse, H.; Hemadi, M.; Djedjat, C.; Yéprémian, C.; Coradin, T.; Couté, A. Cyanobacteria as bioreactors for the synthesis of Au, Ag, Pd, and Pt nanoparticles via an enzyme-mediated route. *J. Nanosci. Nanotechnol.* **2007**, *7*, 2696–2708. [\[CrossRef\]](#) [\[PubMed\]](#)
114. Afzal, B.; Yasin, D.; Husain, S.; Zaki, A.; Srivastava, P.; Kumar, R.; Fatma, T. Screening of cyanobacterial strains for the selenium nanoparticles synthesis and their anti-oxidant activity. *Biocatal. Agric. Biotechnol.* **2019**, *21*, 101307. [\[CrossRef\]](#)
115. Chakraborty, N.; Banerjee, A.; Lahiri, S.; Panda, A.; Ghosh, A.N.; Pal, R. Biorecovery of gold using cyanobacteria and an eukaryotic alga with special reference to nanogold formation—A novel phenomenon. *J. Appl. Phycol.* **2009**, *21*, 145. [\[CrossRef\]](#)
116. Hamouda, R.A.; Hussein, M.H.; Abo-Elmagd, R.A.; Bawazir, S.S. Synthesis and biological characterization of silver nanoparticles derived from the cyanobacterium *Oscillatorialimnetica*. *Sci. Rep.* **2019**, *9*, 13071. [\[CrossRef\]](#)
117. Roychoudhury, P.; Gopal, P.K.; Paul, S.; Pal, R. Cyanobacteria assisted biosynthesis of silver nanoparticles—A potential antileukemic agent. *J. Appl. Phycol.* **2016**, *28*, 3387–3394. [\[CrossRef\]](#)
118. Sonker, A.S.; Richa; Pathak, J.; Rajneesh; Kannaujiya, V.K.; Sinha, R.P. Characterization and in vitro antitumor, antibacterial and antifungal activities of green synthesized silver nanoparticles using cell extract of *Nostoc* sp. strain HKAR-2. *Can. J. Biotech.* **2017**, *1*, 26–37. [\[CrossRef\]](#)
119. Ebadi, M.; Zolfaghari, M.R.; Aghaei, S.S.; Zargar, M.; Shafiei, M.; Zahiri, H.S.; Noghabi, K.A. A bio-inspired strategy for the synthesis of zinc oxide nanoparticles (ZnO NPs) using the cell extract of cyanobacterium *Nostoc* sp. EA03: From biological function to toxicity evaluation. *RSC Adv.* **2019**, *9*, 23508–23525. [\[CrossRef\]](#)
120. Venditto, V.J.; Simanek, E.E. Cancer therapies utilizing the camptothecins: A review of in vivo literature. *Mol. Pharm.* **2010**, *7*, 307–349. [\[CrossRef\]](#)
121. Zhang, Y.S.; Zhang, Y.N.; Zhang, W. Cancer-on-a-chip systems at the frontier of nanomedicine. *Drug Discov. Today* **2017**, *22*, 1392–1399. [\[CrossRef\]](#) [\[PubMed\]](#)
122. Farokhzad, O.C.; Langer, R. Impact of nanotechnology on drug delivery. *ACS Nano* **2009**, *3*, 16–20. [\[CrossRef\]](#) [\[PubMed\]](#)
123. Sun, T.; Zhang, Y.S.; Pang, B.; Hyun, D.C.; Yang, M.; Xia, Y. Engineered nanoparticles for drug delivery in cancer therapy. *Angew. Chem. Int. Ed.* **2014**, *53*, 12320–12364. [\[CrossRef\]](#) [\[PubMed\]](#)
124. Van Elk, M.; Murphy, B.P.; Eufrazio-da-Silva, T.; O'Reilly, D.P.; Vermonden, T.; Hennink, W.E.; Ruiz-Hernandez, E. Nanomedicines for advanced cancer treatments: Transitioning towards responsive systems. *Int. J. Pharm.* **2016**, *515*, 132–164. [\[CrossRef\]](#) [\[PubMed\]](#)

- 
125. Lemoine, V.; Bernard, C.; Leman-Loubière, C.; Clément-Larosière, B.; Girardot, M.; Boudesocque-Delaye, L.; Munnier, E.; Imbert, C. Nanovectorized microalgal extracts to fight *Candida albicans* and *Cutibacterium acnes* Biofilms: Impact of dual-species conditions. *Antibiotics* **2020**, *9*, 279. [[CrossRef](#)] [[PubMed](#)]
  126. Caddeo, C.; Chessa, M.; Vassallo, A.; Pons, R.; Diez-Sales, O.; Fadda, A.M.; Manconi, M. Extraction, purification and nanoformulation of natural phycocyanin (from Klamath algae) for dermal and deeper soft tissue delivery. *J. Biomed. Nanotechnol.* **2013**, *9*, 1929–1938. [[CrossRef](#)] [[PubMed](#)]
  127. Lee, H.U.; Park, S.Y.; Park, E.S.; Son, B.; Lee, S.C.; Lee, J.W.; Lee, Y.C.; Kang, K.S.; Kim, M.I.; Park, H.G.; et al. Photoluminescent carbon nanotags from harmful cyanobacteria for drug delivery and imaging in cancer cells. *Sci. Rep.* **2014**, *4*, 4665. [[CrossRef](#)] [[PubMed](#)]
  128. Khan, M.; Shobha, J.C.; Mohan, I.K.; Naidu, M.U.; Sundaram, C.; Singh, S.; Kuppusamy, P.; Kutala, V.K. Protective effect of *Spirulina* against doxorubicin-induced cardiotoxicity. *Phytother. Res.* **2005**, *19*, 1030–1037. [[CrossRef](#)]
  129. Hassanen, M.R.; Mahfouz, M.K.; Farid, A.S.; Fadlullah, A.H. Biochemical effects of *Spirulina platensis* against oxidative stress caused by doxorubicin. *Benha Vet. Med. J.* **2015**, *28*, 147–154. [[CrossRef](#)]
  130. Hulkoti, N.I.; Taranath, T.C. Biosynthesis of nanoparticles using microbes—A review. *Colloids Surf. B Biointerfaces* **2014**, *121*, 474–483. [[CrossRef](#)]
  131. Salvador-Reyes, L.A.; Luesch, H. Biological targets and mechanisms of action of natural products from marine cyanobacteria. *Nat. Prod. Rep.* **2015**, *32*, 478–503. [[CrossRef](#)] [[PubMed](#)]
  132. Blaha, L.; Babica, P.; Maršálek, B. Toxins produced in cyanobacterial water blooms-toxicity and risks. *Interdiscip. Toxicol.* **2009**, *2*, 36–41. [[CrossRef](#)] [[PubMed](#)]
  133. Mayer, A.M.; Glaser, K.B.; Cuevas, C.; Jacobs, R.S.; Kem, W.; Little, R.D.; McIntosh, J.M.; Newman, D.J.; Potts, B.C.; Shuster, D.E. The odyssey of marine pharmaceuticals: A current pipeline perspective. *Trends Pharmacol. Sci.* **2010**, *31*, 255–265. [[CrossRef](#)] [[PubMed](#)]

**Table S1: Clinical trials involving cyanobacterial-derived compounds, which are recruiting, completed or terminated.**

NCT Number <sup>a</sup>	Official Title	Conditions	Phase	Study Design	Start Date and End Date	Responsible, Country
NCT03664323	Efficacy of Chemotherapy or Chemo-anti-PD-1 Combination After Failed Anti-PD-1 Therapy for Relapsed and Refractory Hodgkin Lymphoma: a Series From Lysa Centers.	Hodgkin Lymphoma	n.a. <sup>b</sup>	Observational Model: Cohort (30 individuals) Time Perspective: Retrospective	January 2018  Completed June 2018	Hospices Civils de Lyon, France
NCT02098512	A Multicenter Pilot Study of Reduced Intensity Conditioning and Allogeneic Stem Cell Transplantation Followed by Targeted Immunotherapy in Children, Adolescents and Young Adults with Poor Risk CD30+ Hodgkin Lymphoma (HL)	Hodgkin Lymphoma	Phase I Phase II	Intervention Model: Single Group Assignment Masking: None (Open Label) Primary Purpose: Treatment	March 2014  recruiting	New York Medical College, USA
NCT02713828	A Phase I/II Study of Glembatumumab Vedotin in Patients With gpNMB-Expressing, Advanced or Metastatic Squamous Cell Carcinoma of the Lung	Squamous Cell Carcinoma of the Lung	Phase I Phase II	Allocation: Non-Randomized Intervention Model: Parallel Assignment Masking: None (Open Label) Primary Purpose: Treatment	April 2016  Terminated September 2018	PrECOG, LLC, USA  Several Institutions in the USA
NCT02487979	A Phase 2 Study of GPNMB-Targeted Antibody-Drug Conjugate, CDX-011 (Glembatumumab Vedotin, CR011-vcMMAE; NSC# 763737), in Recurrent or Refractory Osteosarcoma	Recurrent Osteosarcoma	Phase II	Allocation: N/A Intervention Model: Single Group Assignment Masking: None (Open Label) Primary Purpose: Treatment	February 2016  Completed June 2017	National Cancer Institute, USA
NCT02302339	A Phase 2 Study of Glembatumumab Vedotin, an Anti-gpNMB Antibody-drug Conjugate, as Monotherapy or in Combination With Immunotherapies in Patients With Advanced Melanoma	Melanoma	Phase II	Allocation: Non-Randomized Intervention Model: Single Group Assignment Masking: None (Open Label) Primary Purpose: Treatment	November 2014  Terminated October 2018	Celldex Therapeutics, USA
NCT02363283	A Phase 2 Study of CDX-011 (Glembatumumab Vedotin) for Metastatic Uveal Melanoma	Recurrent Uveal Melanoma; Stage IV Uveal Melanoma AJCC v7	Phase II	Allocation: N/A Intervention Model: Single Group Assignment Masking: None (Open Label) Primary Purpose: Treatment	September 2015  Completed July 2018	National Cancer Institute, USA
NCT01997333	A Randomized Multicenter Pivotal Study of CDX-011 (CR011-vcMMAE)in Patients With Metastatic, gpNMB Over-Expressing, Triple Negative Breast Cancer (The METRIC Study)	Metastatic gpNMB Over-expressing Triple Negative Breast Cancer	Phase II	Allocation: Randomized Intervention Model: Parallel Assignment Masking: None (Open Label) Primary Purpose: Treatment	November 2013  Completed August 2018	Celldex Therapeutics, USA

NCT01156753	A Phase II, Randomized, Multicenter Study of CDX-011 (CR011-vcMMAE) in Patients With Advanced GPNMB-expressing Breast Cancer	Breast Cancer	Phase II	Allocation: Randomized Intervention Model: Parallel Assignment Masking: None (Open Label) Primary Purpose: Treatment	July 2010  Completed November 2012	Celldex Therapeutics, USA
NCT00412828	A Phase I/II Study of CR011-vcMMAE in Subjects With Unresectable Stage III or Stage IV Melanoma	Unresectable Stage III or Stage IV Melanoma	Phase I Phase II	Allocation: N/A Intervention Model: Single Group Assignment Masking: None (Open Label) Primary Purpose: Treatment	June 2006  Completed May 2011	Celldex Therapeutics, USA
NCT00704158	A Phase I/II Study of CR011-vcMMAE in Patients With Locally Advanced or Metastatic Breast Cancer	Breast Cancer	Phase I Phase II	Allocation: N/A Intervention Model: Single Group Assignment Masking: None (Open Label) Primary Purpose: Treatment	June 2008  Completed June 2011	Celldex Therapeutics, USA

<sup>a</sup> NCT, Number Clinical Trials (identifier); b n.a., not applicable. Source “ClinicalTrials.gov” database [1].

1. ClinicalTrials.gov is a database of privately and publicly funded clinical studies conducted around the world. It is a resource provided by the United States National Library of Medicine. Available online: <https://clinicaltrials.gov/> (accessed on December 10<sup>th</sup> 2020).